Qualification of innovative floating substructures for 10MW wind turbines and water depths greater than 50m

Project acronym	LIFES50+
Grant agreement	640741
	Collaborative project
Start date	2015-06-01
Duration	40 months

Deliverable D4.1 Simple numerical models for upscaled design

Lead Beneficiary	USTUTT
Due date	2016-02-29
Delivery date	2016-04-01
Dissemination level	Public
Status	Final
Classification	Unrestricted
Keywords	Floating wind modelling, loads analysis, simplified, optimization
Company document number	Click here to enter text.

The research leading to these results has received funding from the European Union Horizon2020 programme under the agreement H2020-LCE-2014-1-640741.

Disclaimer

Document information

Version	Date	Description	
1	2016-03-01	Draft	
		Prepared by	Lemmer, F.; Müller, K.; Pegalajar-Jurado, A; Borg, M.; Bredmose, H.;
		Reviewed by	Aguirre, G., Landbø, T., Andersen, H.S.
		Approved by	Enter names
2	2016-03-29	Final version for QA before submission to EU	
		Prepared by	Lemmer, F.; Müller, K.; Pegalajar-Jurado, A; Borg, M.; Bredmose, H.;
		Reviewed by	Petter Andreas Berthelsen
		Approved by	Jan Arthur Norbeck
3	2015-04-21	Public version	
		Prepared by	Lemmer, F.; Müller, K.; Pegalajar-Jurado, A; Borg, M.; Bredmose, H.;
		Reviewed by	Enter names
		Approved by	Enter names
		In order to enter a new version row, copy the above and paste into left most cell.	

Authors	Organization
Lemmer, F.	USTUTT
Müller, K.	USTUTT
Pegalajar-Jurado, A.	DTU
Borg, M.	DTU
Bredmose, H.	DTU

Contributors	Organization

Definitions & Abbreviations

1p	One time per rotor revolution
3p	Three times per rotor revolution
AQWA	Potential flow simulation model by Ansys
BEM	Blade Element Momentum
Bladed	Aero-hydro-servo-elastic simulation model by DNV-GL
CPU	Central Processing Unit
DEL	Damage-Equivalent Load
DLC	Design Load Case
DOF	Degree Of Freedom
EOG	Extreme Operational Gust
EQM	Equation of motion
FAST	Aero-hydro-servo-elastic simulation model by NREL
FEM	Finite Element Model
FFT	Fast Fourier Transform
FOWT	Floating Offshore Wind Turbine
HAWC2	Aero-hydro-servo-elastic simulation model by DTU
MIMO	Multiple-input-multiple-output
MSL	Mean Sea Level
NMPC	Nonlinear model-predictive control
OC3	Offshore Code Comparison Collaboration
OC4	Offshore Code Comparison Collaboration Continuation
OC5	Offshore Code Comparison Collaboration Continuation with Correlation
ODE	Ordinary Differential Equation
PI	Proportional-Integral (controller)
PSD	Power spectral density
QuLA	Quick Load Analysis (simplified model by DTU)
RAO	Response Amplitude Operator
RNA	Rotor-nacelle assembly
RWT	Reference Wind Turbine
SIMA	Floating systems simulation model by Marintek
SISO	Single-input-single-output
SLOW	Simplified Low-Order Wind turbine (simplified model by USTUTT)
SoA	State-of-the-Art
SWL	Sea Water Level
TSR	Tip-Speed Ratio
WAMIT	Wave analysis simulation model by MIT
WP	Work Package

Symbols

$\boldsymbol{A}$	Added mass matrix
A_{hp}	Heave plate cross-sectional area
$\boldsymbol{B}$	Radiation damping matrix
$\boldsymbol{B}$	Model input (SLOW)
B_{aero}	Aerodynamic damping coefficient
$\boldsymbol{C}$	Hydrostatic restoring
$\boldsymbol{C}_{moor}$	Linearized mooring system stiffness
C_D	Drag coefficient
c_P, c_T	Aerodynamic power and thrust coefficients
D	Effective platform diameter (for drag force calculation)
EI	Tower bending stiffness
$\boldsymbol{F}$	External force vector

$\boldsymbol{F}_{aero}$	Aerodynamic force
$\boldsymbol{F}_{exc}$	Hydrodynamic wave excitation force
$\boldsymbol{F}_{drag}$	Hydrodynamic drag force
$\boldsymbol{F}_{hydro}$	Hydrodynamic force
f	Frequency
H_F, V_F	Horizontal and vertical fairleads forces
H_s	Significant wave height
i	Imaginary unit
$\boldsymbol{K}$	Radiation impulse response kernel
$\boldsymbol{k}$	Applied forces
k_p	Proportional gain (controller)
$\boldsymbol{M}$	Structural mass matrix
M_{yT}	Tower-base bending moment
m_{top}, m_{bot}	RNA & platform mass, respectively (QuLA)
m_t	Tower mass
$\boldsymbol{P}$	Linearized velocity-dependent forces
$\boldsymbol{p}$	Coriolis, centrifugal and gyroscopic forces
$\boldsymbol{q}$	Generalized coordinates
$\boldsymbol{Q}$	Linearized position-dependent forces
R	Rotor radius
$\dot{r}_{rotor,x}$	Horizontal hub velocity
T_i	Time constant (controller)
T_p	Peak spectral period
t	Time
$\Delta\boldsymbol{u}$	Differential model input
$\boldsymbol{x}$	State vector
x_p	Platform surge displacement
x_t	Tower-top fore-aft displacement
v_0	Rotor-effective wind speed/Mean wind speed
v_{rel}	Relative rotor-effective wind speed
u, w	Horizontal and vertical fluid particle velocity
$\dot{x}, \dot{z}$	Horizontal and vertical platform velocity
x_F, z_F	Horizontal and vertical fairlead displacement
x_{hub}	Horizontal hub displacement
z_p	Platform heave displacement
β_p	Platform pitch displacement
η	Wave elevation
θ	Blade pitch angle
λ	Tip-speed ratio (TSR)
ξ	Generalized rigid-body coordinates of floating body
ρ	Density
ω	Angular frequency
Ω	Rotor speed
Ω_{ref}	Reference (rated) rotor speed

Executive Summary

This deliverable presents parametric design models for an upscaling of the LIFES50+ platforms as well as simplified coupled models. The frequency-domain model QuLA by DTU and the time-domain multibody model SLOW by USTUTT are introduced. The two models feature high computational efficiency, which is beneficial for early conceptual design calculations. Many different load cases can be calculated with QuLA, featuring a real-time factor of more than 1000. This is due to the nature of the frequency-domain description - but even SLOW, written in time-domain, simulates about 160 times faster than real time allowing the designer to run many system simulations and sensitivity studies for early-stage optimization.

Whereas QuLA represents the wind turbine through pre-computed rotor loads and an aerodynamic damping coefficient SLOW uses an actuator-disk-like approach and therefore includes also the blade-pitch angle and thus the effects of the control. QuLA's time-series of the aerodynamic thrust forces can be obtained from state-of-the-art models, run independently of the simplified models. This has the advantage that the detailed simulation model is not necessary for the platform designer, avoiding confidentiality issues. SLOW consists of a nonlinear multibody system, which can be easily adjusted for a new model layout. It uses symbolic programming for easy portability and high computational speed. Various levels of fidelity, like a linearized version besides the nonlinear one allow a comparison of different levels of modeling detail.

The models are compared to simulations of the state-of-the-art tool FAST in a comprehensive study of system identification, fatigue and extreme load cases of the LIFES50+ design basis. One-hour simulations for the whole operating range with three different wave environments are performed and additionally, with the 50-year extreme wave climate. Prior to this, system identification tests are run, checking the transient and steady-state behavior. For this study, a generic concrete semi-submersible platform is used together with the DTU10MW reference wind turbine. A conceptual controller accounting for the floating foundation has been developed for the present deliverable in order to simulate the whole operating range. It includes a common nonlinear state feedback below rated conditions and for above rated-wind speeds, which are critical for floating wind turbines, a proportional-integral controller with gain scheduling. This ensures constant system dynamics of the floating wind turbine throughtout the operating range.

In general, a good agreement can be seen between the simplified models and the reference model in terms of eigenfrequencies, steady states and wave response, proving their consistency. The fatigue loads in operational conditions agree fairly well and can therefore be used for conceptual design calculations. For extreme loads, however, notable deviations occur. One reason for this is the strong nonlinearity of the external aerodynamic and hydrodynamic forces. In the 50-year extreme sea states the rotor experiences extreme inflow conditions, which challenge the simplified models. Here, an application of the simplified models needs to be carefully evaluated. The detailed differences are summarized in a discussion of the model features, their tuning and their applicability across the range of design load cases. The last aspect will be worked on in later deliverables of WP4 in LIFES50+.

Contents

Introduction

Work Package 4 of LIFES50+ examines and develops numerical models of Floating Offshore Wind Turbines (FOWT) in order to first assess accuracy and subsequently improve state-of-the-art methods of the numerical FOWT design practice that has been described in the LIFES50+ deliverables D4.4 and D7.4, see [1] and [2]. The work of the partners in this work package addresses a number of aspects of the numerical design process of floating wind turbines. The results of the specific studies of WP4 will be eventually fed back into general guidelines. This also includes improving simplified design tools, which is the focus of the present report.

The role of simplified numerical models falls within the conceptual design stage of the floating support structure design process, where computational efficiency is paramount to evaluating different configurations in numerous environmental conditions whilst maintaining sufficient accuracy. Numerical models for offshore wind turbines are often divided into decoupled and coupled models, referring to the way the combined loads from the rotor and floater are calculated. In the present report, decoupled conceptual methods using spreadsheet calculations and parametric panel code simulations by the University of Stuttgart are addressed first in Section 1.1 and 1.2. Simplified coupled models are then introduced in Section 1.3. These tools have their origin at the two research partners Technical University of Denmark (DTU) and the University of Stuttgart (USTUTT) and are based on different physical assumptions leading to a different range of applicability.

The models are applied to the generic DTU 10MW offshore reference wind turbine [3] on the generic concrete TripleSpar concept developed in the project INNWIND.EU, see [4]. This concept is used in WP4 until the two LIFES50+ concepts are selected. The load cases considered here have been selected from the LIFES50+ design basis [5] for site C, West of Barra, which presents the most extreme weather conditions in LIFES50+. Through the evaluation of the results from these load cases, the range of applicability and limitations of the simplified design tools herein is identified.

The definition of assumptions with decreasing uncertainty throughout the design process and the concept of increasing the level of fidelity continuously during the design of FOWT is the subject of Chapter 1. In Chapter 2 the reference FOWT considered is introduced. The selection of load cases of this deliverable is topic of Chapter 3 before the results are presented and analysed in Chapter 4. Finally, Chapter 6 provides some key conclusions from the analyses.

1 Modelling Approaches

Modelling tools for FOWT have been improved significantly during the last years. Due to the transient and nonlinear loading from wind and waves, time-domain simulations are usually performed, as opposed to the commonly used frequency-domain methods from the oil and gas industry. There are a number of open-source and commercial software available, which couple aerodynamic models with structural multi-body codes, quasi-static or dynamic mooring line models and time-domain hydrodynamic models. These models normally use Blade Element Momentum (BEM) theory for aerodynamics, modally reduced bodies for the structural multi-body model and the Cummins equation for the hydrodynamics. These models will be called “state-of-the-art” (SoA) tools in this report

The numerical design process does usually not start with these tools as they require a quite detailed description of the overall system. At an early design stage, for upscaling and optimization, simpler models which give a qualitative overview of the feasibility of a concept with low computational cost are suitable. Here, parametric models for spreadsheet design methods and panel code calculations are

presented in Section 1.1 and 1.2. After this, the simplified coupled models are introduced in Section 1.3 – the frequency-domain tool QuLA by DTU in and the simplified coupled model SLOW by USTUTT.

The different design stages of a floating wind turbine system and its components warrant the use of different levels of modelling detail and accuracy in numerical design tools. As observed in responses from questionnaires to concept developers of LIFES50+ in [6], [1], [2] as well as in literature, the simplified numerical models considered in this report provide main results in the first "conceptual design stage", see [2] . Higher fidelity state-of-the-art tools, e.g. FAST, Bladed, SIMA, HAWC2, are then utilized once the whole design space has been explored and a conceptual design has been achieved.

The type and variety of simulated load cases changes as a function of design stage and numerical tools being used. In LIFES50+, one objective is to develop the concept of interconnected design phases, load cases and simulation models. This will provide end users a systematic framework whereby types of simulation models and load cases to consider as a function of design phase are clearly defined. In this report, model verification procedures and load cases to be considered in conjunction with the above described simplified numerical tools are studied.

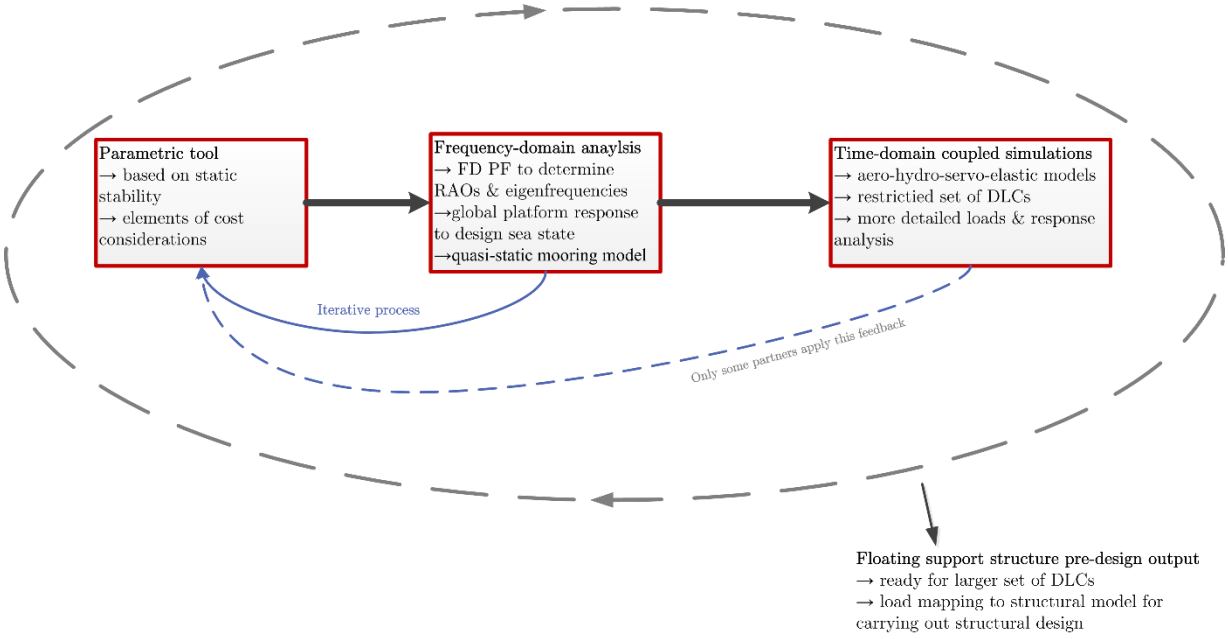

Figure 1 - Numerical design process for FOWT, [6].

The numerical design of floating foundations commonly starts with spreadsheet calculations for the assessment of the hydrostatic properties and addresses response amplitude operators (RAO). These two steps as the initial procedures of the numerical FOWT design process are subject to the next two sections.

1.1 Parametric spreadsheet calculations

In this early design phase the material cost can already be assessed giving a good overview of the feasibility of a selected concept. If these models are set up in a parametric way, sensitivities and distinct properties can be identified early in the design process. Examples are the draft, the material cost related to the hydrostatic and dynamic behaviour. In this section such simple parametric models are illustrated for the TripleSpar foundation, which is used as a generic concept in this deliverable. It is introduced in Section 2.1.

For the concept studies the main constraints with respect to system behaviour (and thus apart from constraints that are imposed on the design by other stages or parts of the project, e.g. fabrication and installation, which is considered to be addressed prior to the concept study) are related to the hydrostatic properties: (1) In vertical direction the buoyancy needs to equal the overall mass, (2) in pitch direction a maximum heeling angle (e.g. between 3 and 7 degrees) is set as a constraint such that all considered designs ensure this heeling angle at rated thrust. See Table 1 for all constraints and variables considered in the presented work.

	Fixed parameters (constraints)	Free variables	Dependent variables	Optimization variables
Spreadsheet	• Buoyancy to support system • Constant heeling angle under rated wind loads.	• Column diameter • Column spacing	• Draft • Tripod wall thickness & diameter	• Material cost • Draft (depending on site + port)
Parametric panel code	• RAO peak period			• Low wave load amplification at wave frequencies

Table 1 - Constraints and optimization variables.

Figure 2 shows the material cost and the draft for different column spacings on the horizontal axis and column radii on the vertical axis. The draft results from the constraints are also included. The draft might be selected based on the site but it might also be defined as an optimization variable in order to target a foundation with low draft, flexible to multiple sites. The assumptions of these calculations are a constant wall thickness of the columns with reinforced concrete. The required steel mass of the tripod has been approximated through static FEM calculations for two designs with linear interpolations for column spacings inbetween.

Although many design steps are omitted here, this example puts the next part on the de-coupled potential flow calculations in order to the subsequent simplified coupled methods.

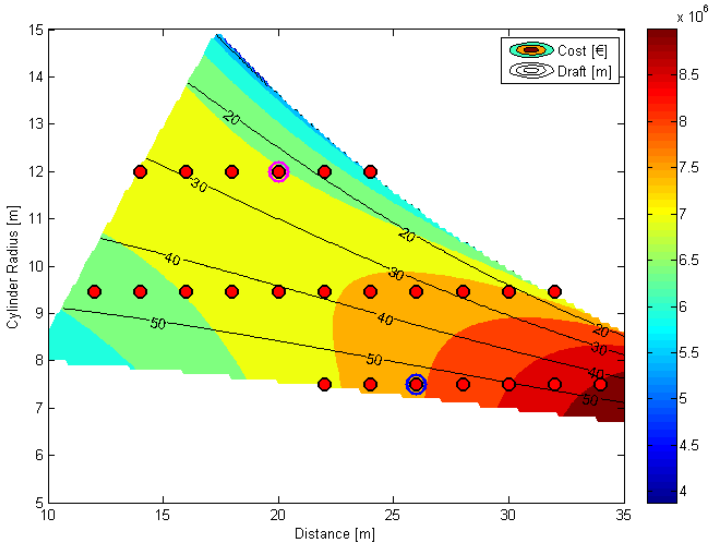

Figure 2 – Spreadsheet studies of TripleSpar platform.

1.2 Parametric panel code calculations

In a second step a subset of the design space displayed in Figure 2 is defined to be the input to panel code calculations. These calculations mainly result in the response amplitude operator (RAO), which is necessary to ensure that the platform resonances are not excited by the waves. Figure 3 shows the calculation mesh of Ansys Aqwa used for the parametric calculations. The results are shown in Figure 4 for different geometries with the draft, the material cost and the peak RAO frequency for a subset of the previous design space. It shows that for design of rather large column diameters (red) the material cost is low but the peak RAO frequencies tend to be too high for common wave spectra. Heave plates have been chosen as an additional design parameter. For some designs a significant increase in peak RAO period is visible.

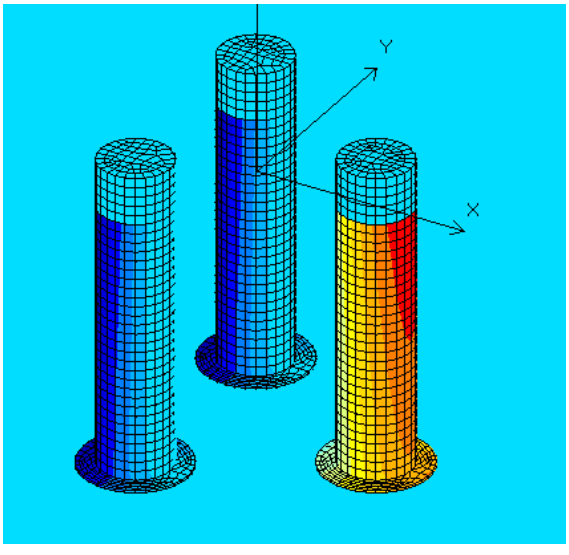

Figure 3 – Mesh in Ansys Aqwa for 1st order radiation and diffraction calculation.

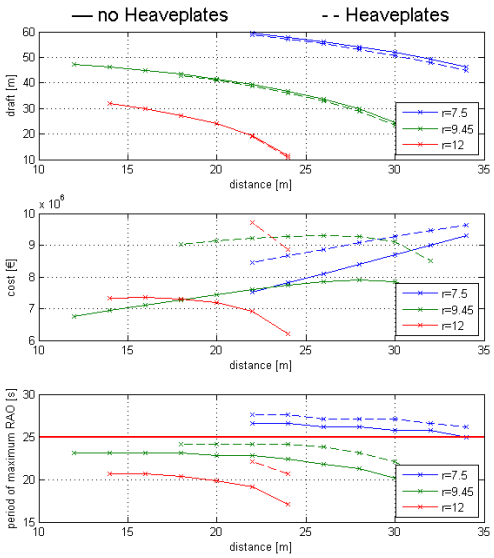

Figure 4 - Draft, cost and maximum RAO period for the reduced design space.

In summary, parametric models provide a suitable overview of the main dimensions and properties to be used for more advanced calculations or as a basis for multi-disciplinary optimization approaches, as long as sufficient accuracy is achieved and all relevant load effects are accounted for.

1.3 Simplified aero-hydro-servo-elastic codes

The next step in the numerical design process after spreadsheet calculations and de-coupled panel code calculations is the coupled motion and loads analysis with simplified models. Here two suitable models are presented: (1) the linear frequency-domain model, **QuLA** is applied and explained in Section 1.3.1. It allows for very high computational speed and is therefore very useful in the early-stage design. (2) **SLOW**, subject of Section 1.3.2 is based on nonlinear symbolic equations, which can be linearized. It has been developed especially for fast loads analysis and controller design, where linear models are necessary for standard control-design approaches.

The prospect of the simplified models presented in this section is a computationally efficient and sufficiently accurate prediction of the motion and loads for an understanding of the dynamic behavior during the conceptual design phase.

1.3.1 QuLA

QuLA is a simple, fast numerical model for the simulation of the dynamic response of the floating wind turbine described in Chapter 2 (see Figure 5), and is suitable for designing the floating foundation. The model solves the equations of motion in the frequency domain and then transforms the response to the time domain using Fast Fourier Transform (FFT). In the present setup for a FOWT, and after pre-computation of rotor loads and hydrodynamic coefficients in e.g. WAMIT, QuLA performs with a ratio of simulated time to CPU time of around 1400 for a 1-hour simulation and a time step of 0.025 s on a standard PC, which makes it very suitable for pre-design or conceptual design and design optimization.

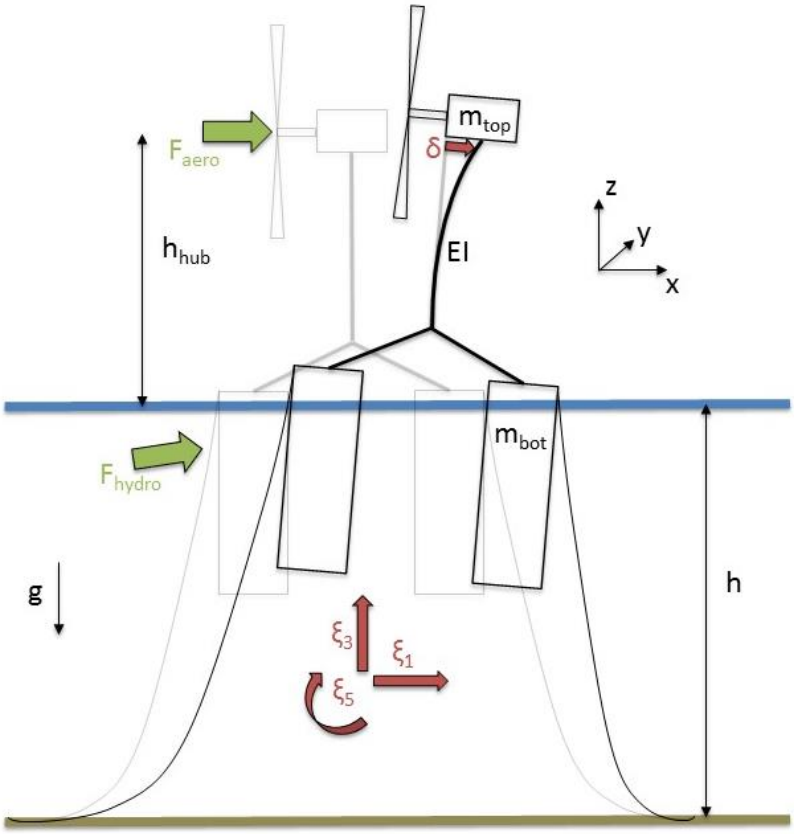

Figure 5: Sketch of the FOWT as implemented in QuLA

In the model, the floating wind turbine is simplified into two concentrated masses, m_{top} and m_{bot} and the tower. The top mass m_{top} includes the wind turbine rotor, hub and nacelle, while m_{bot} refers to the floating platform. The tower is modelled as a flexible Euler beam with distributed mass per length m_t and distributed bending stiffness *EI*, and is only allowed to bend according to its first fore-aft modal shape. Four degrees of freedom are defined and solved for: floater surge x_p, floater heave z_p, floater pitch β_p around the floatation point and the elastic deflection at the tower top, x_t. The time-domain response of the floating wind turbine is governed by the equation of motion [7]:

$$(\boldsymbol{M}+\boldsymbol{A})\ddot{\boldsymbol{x}}(t)+\int_0^t \boldsymbol{K}(t-\tau)\dot{\boldsymbol{x}}(\tau)d\tau+\boldsymbol{C}\boldsymbol{x}(t)=\boldsymbol{F}(t) \quad (1)$$

Where $\boldsymbol{M}$ is the inertia matrix of the structure, $\boldsymbol{A}$ is the hydrodynamic added mass, the convolution integral represents the linear radiation damping and $\boldsymbol{C}$ is the hydrostatic restoring matrix. $\boldsymbol{F}(t)$ is the vector of external forcing of the four DOFs due to wind and waves, namely $\boldsymbol{F}_{aero}$ and $\boldsymbol{F}_{hydro}$. The vector $\boldsymbol{x}(t)$ represents the motion in the different degrees of freedom. If harmonic motion is assumed, then one can write the motion as $\boldsymbol{x}(t) = \boldsymbol{x}(\omega)e^{i\omega t}$ and the equation of motion can be written in frequency domain:

$$(-\omega^2(\boldsymbol{M}+\boldsymbol{A}(\omega))+i\omega\boldsymbol{B}(\omega)+\boldsymbol{C})\boldsymbol{x}(\omega)=\boldsymbol{F}(\omega) \quad (2)$$

Here the added mass and damping matrices, $\boldsymbol{A}$ and $\boldsymbol{B}$, depend on frequency. Once the equation is solved in frequency domain, the response in the time domain can be obtained by inverse Fast Fourier Transform (iFFT).

1.3.1.1 Hydrodynamics

1.3.1.1.1 Wave kinematics

Under the assumption of inviscid, incompressible and irrotational flow, the linear Airy wave theory provides a quick and simple estimation of the wave kinematics in constant water depth. Although more complex wave theories could provide a more precise description of the flow, they would also increase the computational cost, compromising the speed of the simple models. Thus, for the initial phases of the design process, where efficiency is preferable over accuracy, linear Airy theory is applied.

1.3.1.1.2 Hydrodynamic loads

Given the geometry and size of the floating platform, a slender body approach and the consequent application of the Morison equation for the hydrodynamic loads may not be sufficient. Instead, radiation and diffraction effects must be included in the modelling of wave-structure interaction. For this purpose, the commercial numerical tool WAMIT is employed. WAMIT solves the wave-structure interaction in frequency domain by use of a potential flow panel method. For the present model, the WAMIT tool is used to obtain the added mass and damping matrices $\boldsymbol{A}(\omega)$ and $\boldsymbol{B}(\omega)$, as well as the hydrostatic restoring matrix $\boldsymbol{C}$ and the wave excitation forces $\boldsymbol{F}_{exc}(\omega)$, due to incident wave (diffraction and wave scattering). Inherent to potential flow methods, viscous effects are not included in the WAMIT computations. Hence, empirically-determined viscous damping is added to the system through the damping matrix $\boldsymbol{B}$, and the viscous forcing in surge and heave directions is modelled through the drag term in the Morison equation:

$$F_{drag,x}(t) = \int_z \frac{1}{2}\rho_w C_{Dx} D(u - \dot{x})|u - \dot{x}|dz \tag{3}$$

$$F_{drag,z}(t) = \frac{1}{2}\rho_w C_{Dz} A_{hp}(w - \dot{z})|w - \dot{z}| \tag{4}$$

where ρ_w is the water density, C_D are the drag coefficients, D is the cylinder diameter, A_{hp} is the cross-area of a heave plate, u and w are the horizontal and vertical wave velocities, and $\dot{x}$ and $\dot{z}$ denote the structure velocities in surge and heave directions, respectively. The viscous forces are computed in the time domain and transformed to the frequency domain. Hence, the total hydrodynamic force to be included in the equation of motion would be:

$$\boldsymbol{F}_{hydro}(\omega) = \boldsymbol{F}_{exc}(\omega) + \boldsymbol{F}_{drag}(\omega) \tag{5}$$

1.3.1.2 Aerodynamics

1.3.1.2.1 Wind field

The turbulent wind field for each wind speed is precomputed using TurbSim, an open-source numerical tool to create stochastic inflow turbulence, developed at the National Renewable Energy Laboratory (NREL). The wind fields are created from a Kaimal spectrum, for a turbulence class C according to the IEC-61400-3 standard. The grid, centered in the hub, spans 230 m and 33 points in the vertical and horizontal directions, to ensure that the rotor area is well covered even when large platform motions occur.

1.3.1.2.2 Aerodynamic loads

In order to capture the complex rotor aerodynamics and at least some of the effects of the controller while keeping the numerical model fast and simple, the aerodynamic loads and aerodynamic damping are precomputed with FAST, an open-source integrated numerical tool developed at the National Renewable Energy Laboratory (NREL). For each wind speed, a simulation in turbulent wind is run with rigid foundation and tower, and time series of aerodynamic loads are stored. Next, another simulation is run for the same wind speed, where the platform pitch is enabled and an initial pitch displacement is imposed. The amplitude of the hub displacement will decay in time due to the aerodynamic damping, as seen in Figure 6 (left). The exponential decay of the peaks is used to compute the aerodynamic damping for the given wind speed. The same procedure is repeated for different wind speeds and a value of aerodynamic damping is extracted in each case (see Figure 6 (right)).

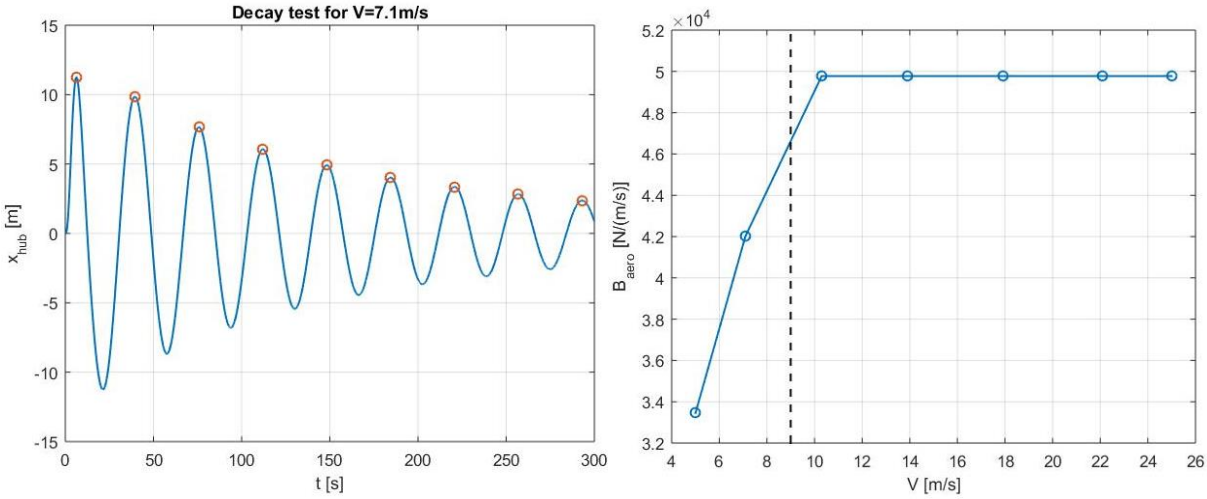

Figure 6: Free pitch decay test in wind (left) and aerodynamic damping as a function of wind speed (right)

The aerodynamic loads precomputed with FAST are applied to the simple model as $\boldsymbol{F}_{aero}$. The aerodynamic damping is included in the equation of motion through the linear damping matrix $\boldsymbol{B}$. However, since the wind turbine controller was originally tuned for an onshore turbine, for wind speeds near or above rated the pitch motion in the decay test will become unstable. Therefore, and as a temporary solution until the controller for floating application is public, the aerodynamic damping for wind speeds above 9 m/s was conservatively extrapolated from the values obtained for 5 and 7.1 m/s, as seen in Figure 6.

1.3.1.3 Mooring system

The mooring system consists of 3 catenary lines, as specified in Section 1.3.1.3. In order to avoid solving the position of the catenary lines in time, the mooring system in the simple model is replaced by a linear mooring matrix $\boldsymbol{C}_{moor}$, obtained at the equilibrium position and added to the original hydrostatic restoring matrix $\boldsymbol{C}$. Although a drastic simplification, the linearization of the mooring system provides simplicity and speed to the simple model.

1.3.1.4 Setup of the model

In order to adapt the QuLA model to another floating wind turbine, one needs the following elements:

- Hydrodynamic data such as hydrostatic, added mass and radiation damping matrices for the given floating platform (computed with WAMIT or similar software)
- Linearized mooring matrix for the given mooring configuration

- State-of-the-art model of the land-based wind turbine (in e.g. FAST) from which to extract the aerodynamic loads and the aerodynamic damping

1.3.1.5 Calibration of the model

The simple model was calibrated against a FAST version of the same floating wind turbine. Time series of decay tests in surge, heave and pitch were produced with FAST and used as reference for calibration. The natural frequencies were matched by adjusting the mooring matrix $\boldsymbol{C}_{moor}$, while the linear damping matrix $\boldsymbol{B}$ was tuned to obtain the desired damping ratios. Further adjustment of the hydrostatic matrix $\boldsymbol{C}$ was necessary in order to match the full aero-elastic model. For the present results, the pitch diagonal element of the hydrostatic restoring matrix ($\boldsymbol{C}_{55}$) was reduced by 16% in order to match the pitch natural frequency. It is expected that the cause of this need can be found by closer investigations.

1.3.2 SLOW

The simplified FOWT model SLOW (Simplified Low-Order Wind turbine) developed at the University of Stuttgart aims at a fast simulation of the overall nonlinear coupled dynamics. So far, simplified, computationally efficient models allowing for numerous iterations at an early stage of development are not possible with state-of-the-art, commercially available software. Simulation outputs to focus on here are, e.g., the unconstrained 3D platform motion, rotor speed, blade pitch angle, tower top displacement and main internal forces. With the linearized from of the equations of motion also the eigenvalues and eigenvectors can be analysed. Load distributions or specific node deflections of certain bodies on the other hand are not sought to be covered by this model. The simplification also implies that higher frequency modes of the stiffer DOFs like the blades or generator shaft are not considered. From a numeric point of view focus is set on computational speed so that iterations, recursions, integrations, excessive memory access, etc. is avoided wherever possible. In order to accomplish these goals, the structure is modelled as a coupled multibody system of rigid bodies with only four DOFs. The equations of motion (EQM) of the 3D model are set up by applying the Newton-Euler formalism. As a result the mathematical model is available in state-space formulation as a system of symbolic ordinary differential equations (ODE), which can be directly compiled, yielding a high computational efficiency. Aerodynamics as well as the mooring line model is based on an interpolation of look-up data that is gained in a pre-processing step. Aerodynamic coefficients allow the calculation of rotor torque and thrust with a scalar rotor-effective wind speed as input. Quasi-static fairlead forces from the mooring lines as a function of horizontal and vertical displacements are stored offline and interpolated during runtime. Hydrodynamic forces are computed by the reduced model through a potential flow approach.

The necessary pre-processing steps to run SLOW are (1) the identification of the force-RAO (wave excitation force vector), the added mass and damping through a panel code. This calculation takes roughly 10min per frequency-point with Ansys-Aqwa for the model used here. (2) The quasi-static mooring force-discplacement relationship needs to be calculated which takes only seconds. (3) For the calculation of the aerodynamic forces on the rotor disk the power and thrust coefficients have to be calculated over tip-speed ratios (TSR) and blade pitch angles. This takes about three hours for the model used here.

The simulation to CPU-time ratio has been determined for a 1-hour simulation with a fixed time-step of 0.025s and a 4th order Runge-Kutta solver, it is about 160.

Table 2 shows the main characteristics of the model.

Table 2 - SLOW main properties

Number of DOFs	4 (in this work)
Structural model	Flexible multibody system, modally reduced bodies, floating frame of reference. Nonlinear/linear
Hydrodynamic model	Panel code (pre-processing) with constant added mass, linear damping (in this work), state-space wave excitation force model
Aerodynamic model	Look-up table of power- and thrust coefficient, nonlinear/linear, relative, rotor-effective wind speed, blade-pitch-dependent
Mooring line model	Nonlinear, quasi-static
Wind turbine controller	Torque and pitch control
Sim. Time/CPU time	160
Programming	C, Matlab

The next subsections will first introduce the set-up of the EQM of the structure and then addressing the aero- and hydrodynamic subsystems.

1.3.2.1 Wind turbine structural model

Figure 7 shows a sketch of the exemplary mechanical model of the OC3-Hywind FOWT, as defined in [8]. The EQM are set up from a physical perspective following the Newton-Euler formalism. The thereby involved operations of matrix algebra are calculated with symbolic programming so that the EQM are finally available as ordinary differential equations in a symbolic formulation. The resulting code can then be compiled and thus allows for high flexibility since it can be simulated by standard integration schemes. The state vector $\boldsymbol{x}$, which consists of the vector of the degrees of freedom $\boldsymbol{q}$ and its derivative $\dot{\boldsymbol{q}}$ is here selected as $\boldsymbol{q} = [x_p, \beta_p, x_t, \Omega]^T$ as platform surge and pitch displacement, tower-top fore-aft displacement due to deformation and the rotor speed. This is a minimal set of DOFs which allows to obtain a good overview of the main dynamics and as a tool for controller design. The nonlinear EQM can be transformed into state space domain

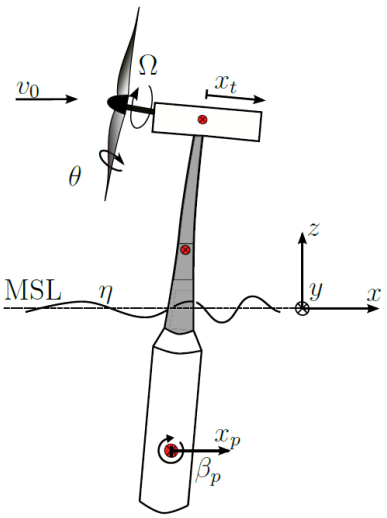

Figure 7 - Sketch of SLOW FOWT model.

$$\dot{\boldsymbol{x}} = \begin{bmatrix} \dot{\boldsymbol{q}} \\ \ddot{\boldsymbol{q}} \end{bmatrix} = \begin{bmatrix} \dot{\boldsymbol{q}} \\ \boldsymbol{M}^{-1}(\boldsymbol{p}(\boldsymbol{q}, \dot{\boldsymbol{q}}) - \boldsymbol{k}(\boldsymbol{q}, \dot{\boldsymbol{q}}, \ddot{\boldsymbol{q}})) \end{bmatrix}. \tag{6}$$

On the right hand side remains the generalized mass matrix $\boldsymbol{M}$, the generalized vector of Coriolis, centrifugal, and gyroscopic forces $\boldsymbol{p}$ and the generalized vector of the applied forces $\boldsymbol{k}$. A more detailed description of the structural model can be found in [9] and [10].

The symbolic equations of (6) can be linearized about an operating point $\boldsymbol{x}_0$

$$\boldsymbol{x} = \boldsymbol{x}_0 + \boldsymbol{\Delta x}. \tag{7}$$

With the position-dependent terms Q and the velocity-dependent terms P and the input matrix $\boldsymbol{B}$ eqn. (6) remains as

$$\begin{bmatrix} \Delta\dot{\boldsymbol{x}} \\ \Delta\ddot{\boldsymbol{x}} \end{bmatrix} = \begin{bmatrix} \boldsymbol{0} & \boldsymbol{E} \\ \boldsymbol{M}^{-1}\boldsymbol{Q} & \boldsymbol{M}^{-1}\boldsymbol{P} \end{bmatrix} \begin{bmatrix} \Delta\boldsymbol{x} \\ \Delta\dot{\boldsymbol{x}} \end{bmatrix} + \boldsymbol{B}\Delta\boldsymbol{u}. \tag{8}$$

The aerodynamic and mooring line forces are here also represented in a linear way. See [11] for details. In the following the nonlinear force models are presented.

1.3.2.2 Aerodynamic model

For this model BEM theory is avoided as this requires an iteration to find the induction factors. The chosen procedure is to simulate a BEM model for various tip-speed ratios λ and blade pitch angles Θ until a steady state is reached as a pre-processing step, see Figure 8. With the resulting two-dimensional look-up table for the thrust and torque coefficients c_T and c_P only the rotor effective wind speed is necessary to calculate the thrust force F_{aero} and torque M_{aero} on the rotor. In order to compute this representative wind speed at hub height first, a weighted average of the three-dimensional turbulent wind field on the whole rotor plane is needed, given by v_0. Second, a transformation of this estimation into the rotor coordinate system is necessary, so that the relative horizontal wind speed is computed. Finally, the relative rotor effective wind speed takes the form

$$v_{rel} = v_0 - \dot{r}_{rotor,x}. \tag{9}$$

This is the scalar disturbance necessary to calculate the thrust force

$$F_{aero} = \frac{1}{2}\rho\pi R^2 c_T(\lambda, \Theta) v_{rel}^2 \tag{10}$$

and the external aerodynamic torque acting on the rotor body

$$M_{aero} = \frac{1}{2}\rho\pi R^3 \frac{c_P(\lambda, \Theta)}{\lambda} v_{rel}^2 \tag{11}$$

with air density ρ and rotor radius R. The described method has already been tested and successfully implemented for nonlinear model predictive control (NMPC) in [12] .

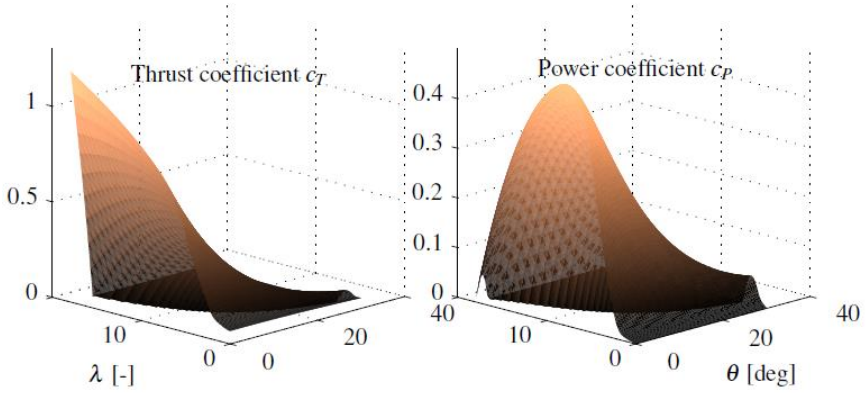

Figure 8 – Example thrust and power coefficient look-up tables identified with AeroDyn [13].

1.3.2.3 Hydrodynamic model

The hydrodynamic model uses constant hydrodynamic coefficients for the added mass and damping.

$$(\boldsymbol{M} + \boldsymbol{A}(\omega_c)\ddot{\boldsymbol{\xi}} + \boldsymbol{B}(\omega_c)\dot{\boldsymbol{\xi}} + \boldsymbol{C}\boldsymbol{\xi} = \boldsymbol{F}_{exc} \tag{12}$$

Morison equation is implemented but has not been enabled for the simulations presented here. The wave excitation force is calculated based on the results of a panel code. The wave excitation force F_{exc} results from an inverse Fourier transform of the wave spectrum multiplied by the frequency-dependent wave excitation force vector (force-RAO) of the panel code.

1.3.2.4 Mooring line model

The floating platform is moored by three catenary lines that are anchored on the seabed. The differential equation for a stationary line is solved analytically. According to [7] the resulting nonlinear system of equations for the horizontal displacement x_F and the vertical displacement z_F of the fairleads with the corresponding horizontal force H_F and the vertical force V_F has the form

$$\begin{aligned} x_F &= f(H_F, V_F) \\ z_F &= f(H_F, V_F). \end{aligned} \tag{13}$$

Applying a numerical solver, the forces on the fairleads can be obtained for various displacements x_F and z_F. Eventually, a function interpolates this data and returns the external forces on the platform body during runtime. Figure 9 shows the force-displacement lookup table.

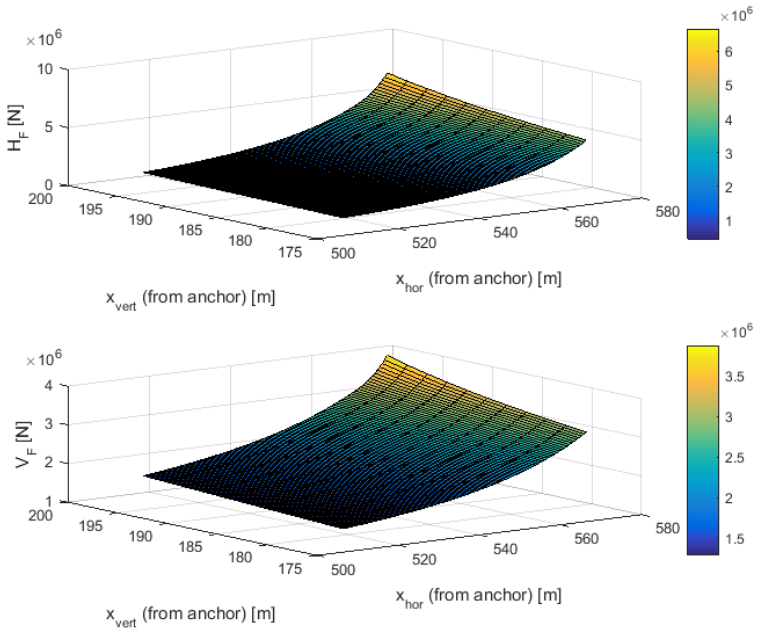

Figure 9 – SLOW nonlinear quasi-static mooring forces.

2 Reference turbine and floating platform

At the delivery date of this report the two public concepts of LIFES50+ have not yet been selected. Therefore, WP 4 uses a generic platform concept together with the DTU10MW reference turbine, [3]. The generic platform concept has been developed by Task 4.3 of the project INNWIND.EU (2012-2017), see [4].

Figure 10 - DTU 10MW Reference Wind Turbine [3]

2.1 Platform

The chosen platform is a semisubmersible platform with three concrete cylinders. The columns are connected by a steel tripod which supports the tower of the DTU 10MW reference wind turbine. The turbine tower has to be shortened by 25 m because of the height of the tripod and the column elevation above sea water level (SWL). The hollow columns are filled with solid ballast. A detailed description of the model can be found in INNWIND.EU deliverable D4.37, [4].

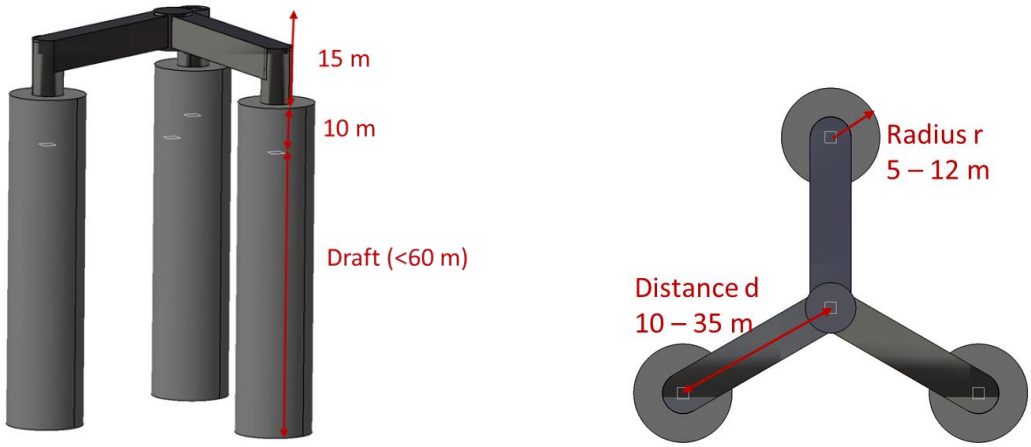

Figure 11 - Platform geometry.

Figure 11 shows the platform geometry. The concrete spar elevation above SWL is 10 m to avoid green water loads on the steel structure. The column radii are of 15m and the column distance to the vertical centerline is 26m (Figure 11). The wall thickness of the concrete columns was set to 0.4 m. The detailed platform properties are collected in Table 3. The advantages of this concept are the low material cost due to easily manufacturable concrete columns with only one interface at their top, above water level. The draft can be adjusted to the selected site and also the installation strategy can be selected according to the available facilities. For low drafts the turbine can be installed in the harbour.

In order to assess the sensitivities of this concept towards material cost and dynamic properties (RAOs) a parametric design approach starting with conceptual spreadsheet calculations up to panel code calculations has been done. This approach is detailed in Section 1.1. The generic concept has been developed specifically for research and optimization studies.

Figure 12 – Two example design of generic TripleSpar concept.

Table 3 - TripleSpar properties.

Platform	Draft	54.46 m
	Elevation of tower base above SWL	25 m
	Water displacement	29 205.09 m^3
	Center of mass below SWL	36.02 m
	Center of buoyancy below SWL	27.54 m
	Platform mass	28 230 t
	Ballast mass	17 264 t
columns	Length	65 m
	Distance to the center	26 m
	Diameter	15 m
	Elevation above SWL	10.5 m
Heave plates	Thickness	0.5 m
	Diameter	22.5m
	Mass	678.7t
Tripod	Total height	15 m
	Height outer cylinder	11 m
	Diameter outer cylinder	5.64 m
	Bar cross-section width	5.64 m
	Wall thickness	0.056 m
	Mass	971.3 t
DTU 10MW RWT	Tower height above SWL	119 m
	Reduced tower length to	94 m

	hub height	
	Rotor diameter	178.3 m
	Rotor mass	228 t
	Nacelle mass	446 t
	Reduced tower mass	433 t
	I_{11} about turbine CM	1.613e9 kgm^2
	I_{22} about turbine CM	1.613e9 kgm^2
	I_{33} about turbine CM	0.491e9 kgm^2
Densities	Concrete density	2 750 kg/m^3
	Steel density	7 750 kg/m^3
	Ballast density	2 500 kg/m^3
	Water density	1 025 kg/m^3
	Total platform mass	28268.22 t
Moments of Inertia about center of mass	Platform I_{11} without turbine	1.8674e10 kgm^2
	Platform I_{22} without turbine	1.8674e10 kgm^2
	Platform I_{33} without turbine	2.0235e10 kgm^2
	FOWT System I_{11}	3.907e10 kgm^2
	FOWT System I_{22}	3.907e10 kgm^2
	FOWT System I_{33}	3.1129e10 kgm^2
Hydrostatics/Hydrodynamics	Heave stiffness C_{33}	5.321e6 N/m
	Pitch stiffness C_{55}	2.922e9 Nm/rad
	Pitch stiffness C55 w/o gravitation (FAST)	-6.199e9Nm/rad

2.2 Mooring system

A catenary mooring system is utilized for station-keeping of the platform. It consists of three lines, with one line per platform column and two upwind lines. The line is connected to a fairlead that extends radially from the column and has a portion lying on the seabed to ensure there are no vertical forces on the anchor in ultimate limit state conditions. Figure 13 depicts the configuration of a single mooring line and Table 4 provides the relevant information concerning the mooring system. Table 5 and Table 6 provide the linearized mooring system stiffness matrices at equilibrium and at rated wind speed positions, respectively, which are used within QuLA and the linear version of SLOW. Details of the mooring design can be found in [14].

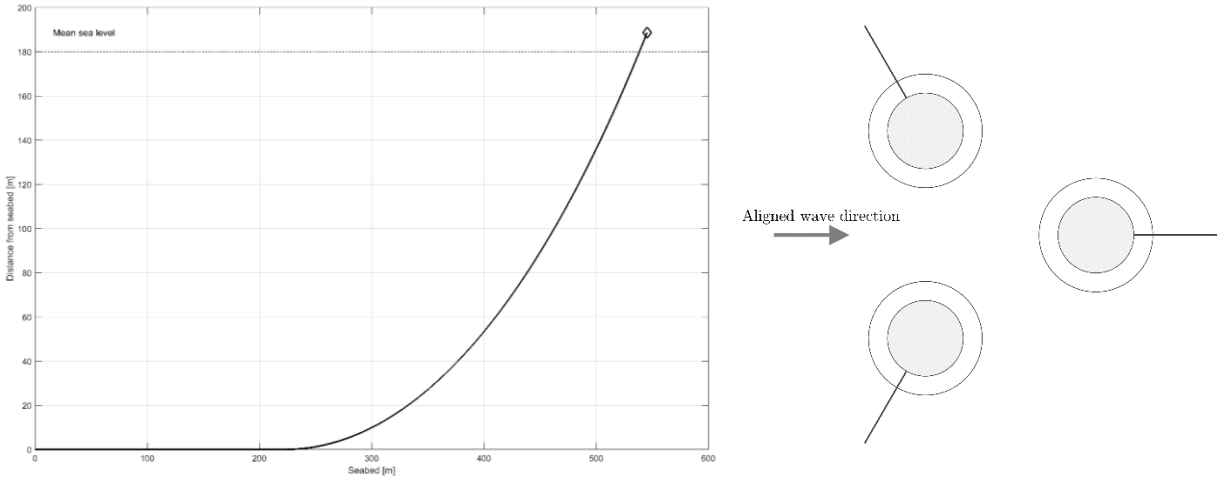

Figure 13 – Left: mooring line configuration, right: mooring system orientation

Table 4 - Mooring system parameters

Parameter	**Unit**	
Number of lines	-	3
Line type	-	Steel chain
Line mass in air	kg/m	594.00
Line mass in water	kg/m	516.59
Chain diameter	m	0.18
Hydrodynamic chain diameter	m	0.31
Un-stretched line length	m	610.00
Extensional stiffness	N	1.3739e+09
Fairlead radius	m	54.48
Anchor radius	m	600.00
Vertical fairlead distance above MSL	m	8.70
Vertical anchor distance below MSL	m	180.00

Table 5 - Linearized mooring system stiffness matrix at equilibrium position [N/m]/[Nm/rad]

	1	2	3	4	5	6
1	-8,3283E+04	4,0571E-05	5,8208E-11	5,6087E-03	-2,8465E+06	6,3033E-07
2	-3,2045E-05	-8,3283E+04	1,1642E-10	2,8455E+06	0,0000E+00	3,6908E-07
3	3,5123E+00	3,7591E-05	-5,7337E+04	4,6545E-03	9,3746E+02	0,0000E+00
4	1,2370E-03	2,8436E+06	0,0000E+00	-1,9999E+08	1,4230E-07	3,2756E-04
5	-2,8436E+06	1,3773E-03	-3,7253E-09	1,8942E-01	-2,0002E+08	-5,672E-04
6	-5,5507E-07	7,6525E+01	0,0000E+00	-1,5652E+05	0,0000E+00	-2,693E+08

Table 6 - Linearized mooring system stiffness matrix at rated wind speed position [N/m]/[Nm/rad]

	1	2	3	4	5	6
1	-7,6888E+04	9,6709E-04	-2,2646E+04	-9,0522E-04	-2,5166E+06	-3,309E-02

2	3,8181E-03	-1,2583E+05	-6,6702E-03	3,9710E+06	4,4467E-09	-9,747E+04
3	-2,2613E+04	7,3521E-04	-5,9279E+04	4,6391E-03	-5,9261E+05	-2,068E-02
4	-1,2496E-01	3,9680E+06	2,1934E-01	-2,8004E+08	1,4230E-07	4,4389E+07
5	-2,5152E+06	2,8448E-02	-5,9427E+05	1,1805E-01	-1,6750E+08	-1,257E+00
6	7,8451E-03	-9,6254E+04	-1,3039E-02	-6,7942E+06	-7,1148E-08	-3,076E+08

2.3 Wind turbine

The DTU 10MW Reference Wind Turbine [3], depicted in Figure 10, is installed on the Triple Spar platform. To account for the freeboard of the platform and to maintain the same hub height the turbine tower was shortened from 115.63 metres to 90.63 metres. This was done by removing the bottom 25 metres of the original tower as detailed by [4]. The influence of this was to increase the tower bending natural frequencies, possibly into the operating 3P range, and should be evaluated further in the conceptual substructure development. However this was not investigated in detail here as the scope of this report is to compare numerical models simulating a reference floating wind turbine design.

2.4 Controller

The DTU10MW reference turbine is here installed on a floating platform. Therefore, the baseline controller cannot be used here due to the "negative damping" problem, which has been reported in the literature, see e.g. [15], [16], [17]. In LIFES50+ a controller will be developed for a floating foundation by DTU. However, this controller was not available before the delivery date of the present report.

Therefore, a conceptual controller has been developed at the University of Stuttgart in order to be able to compare responses at above-rated operational wind conditions. In this section a preliminary controller is designed using a coupled linear model for the above-rated controller and the below-rated control concept adapted from the NREL 5MW RWT [18]. For the purpose of designing a simple conceptual controller a single-input-single-output (SISO) Proportional-Integral (PI) controller was chosen, see Figure 14. It has been designed using the linearised SLOW model following the method reported in [11]. The design strategy is based on the platform pitch mode: Its pole in the closed loop is set such that its real part is at -0.005 in the left-half plane for all wind speeds. This method results in a gain-scheduling which ensures the stability of the platform at all operating conditions. With this platform pitch mode close to the imaginary axes a good performance of the drivetrain mode is ensured since this mode becomes more stable for increasing gains, which, in turn, lead to instability of the platform, see Figure 16. Figure 15 shows that for two large gains there appears a right-half-plane zero next to the platform pitch mode. For more details see [11].

Figure 17 shows the gain scheduling of the proportional gain of the controller. The time constant is $T_I = 10$s, the generator torque is constant in region 3 (above rated wind speeds).

In the SLOW and FAST model a linear 2nd-order actuator model has been used with a natural frequency of 1.6Hz and a damping ratio of 0.8.

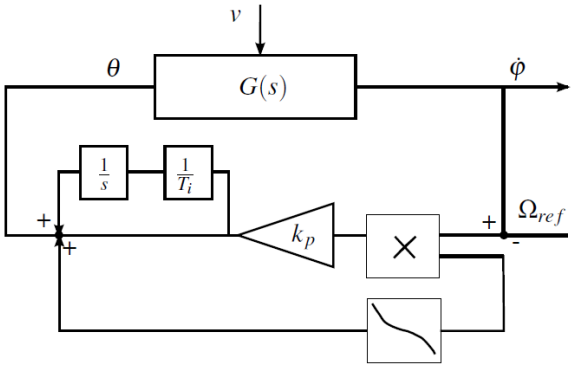

Figure 14 – Conceptual blade-pitch controller.

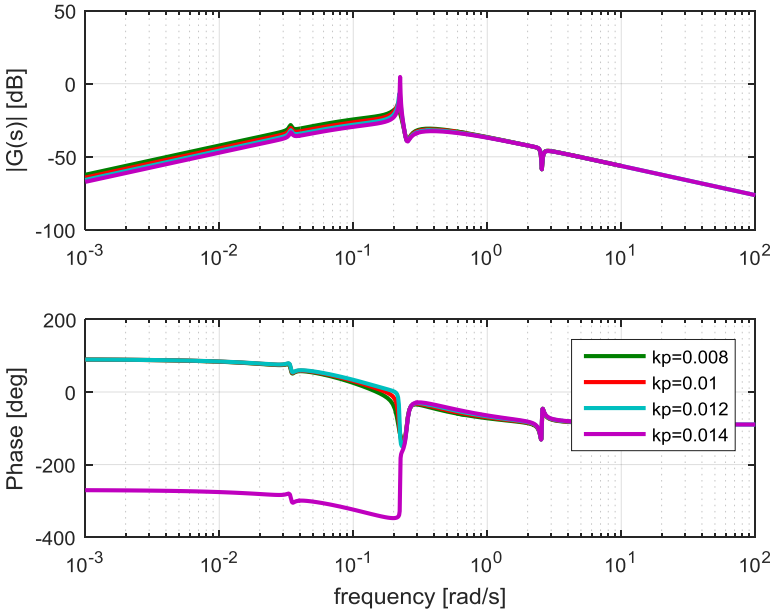

Figure 15 – Closed-loop bode plots from wind speed to rotor speed.

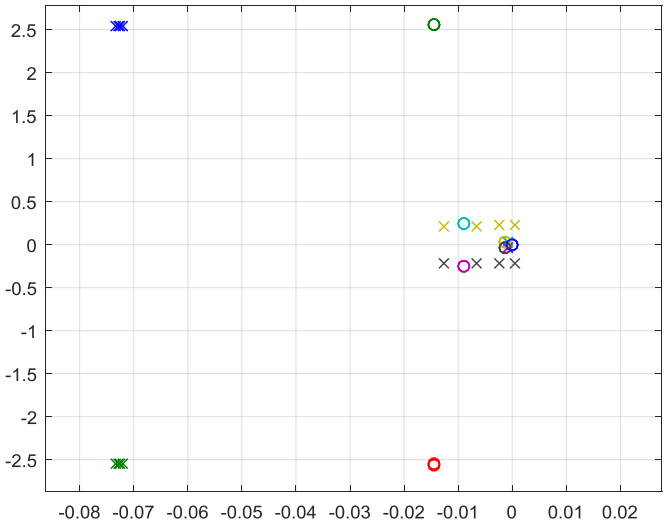

Figure 16 – Closed-loop pole-zero map.

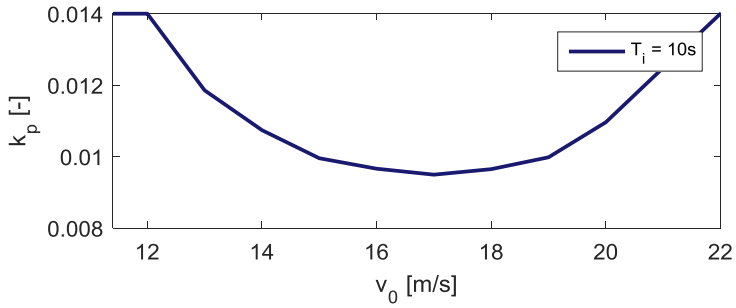

Figure 17 – Gain scheduling of conceptual controller.

3 Selection of Load Cases

A set of simplified, unidirectional load cases is chosen in order to compare the performance of the simple models presented in this document. First, a number of system-identification load cases is selected. This set is derived from the code-comparison projects OC3, OC4 and OC5, see, e.g., [8], [19] and [20]. Especially for model verification these free-decay cases and cases with only wind or only waves are very useful. In this study the simplified models is compared to a common FAST [21] model, see [22] for a description of the model setup. These cases are shown in this report in order to show the agreement of the simple models compared to the reference model FAST in this system identification environment. This allows to better interpreting the results of the design load cases (DLC) in operational and extreme conditions.

3.1 System identification

These cases are necessary in the pre-design phase or every time a new numerical model is set up. It serves for verification of the new setup for plausibility.

Table 7 - Description of cases for system identification

Static equilibrium	Free decay in surge	Free decay in heave	Free decay in pitch	Response to deterministic waves
A case with no wind or waves, to ensure the structure can remain in equilibrium in absence of external loads.	A case with no wind or waves, where the initial surge displacement is +22 m.	A case with no wind or waves, where the initial heave displacement is +6 m.	A case with no wind or waves, where the initial pitch displacement is +8 deg.	Response to a deterministic regular wave with wave height H=6 m and wave period T=10 s.

3.2 Design load cases

Six load cases were selected for this study, in which all considered unidirectional wind and wave conditions to ensure fast evaluation.

3.2.1 Fatigue loads during operation

A set of load cases belonging to DLC1.2, with normal turbulence class C and normal sea states, for the combinations (v_0,H_s,T_p) given in the design basis of LIFES50+ [5] (Table 19) was applied. There are three wave conditions for every wind speed with a different probability of occurrence. The conditions with the smallest peak spectral period T_p are here denoted *A*, and the subsequent ones *B* and *C* in the following.

Table 8 - Environmental conditions for DLC 1.2, extracted from D7.2 [5].

V_{hub} [m/s]	H_s [m]	T_p [s]	Probability
5	1.38	7	6.89%
5	1.38	11	3.45%
7.1	1.67	5	5.99%
7.1	1.67	8	11.98%
7.1	1.67	11	5.99%
10.3	2.2	5	6.41%
10.3	2.2	8	12.83%
10.3	2.2	11	6.41%
13.9	3.04	7	5.12%
13.9	3.04	9.5	10.24%
13.9	3.04	12	5.12%
17.9	4.29	7.5	2.90%
17.9	4.29	10	5.81%
17.9	4.29	13	2.90%
22.1	6.2	10	0.94%
22.1	6.2	12.5	1.88%
22.1	6.2	15	0.94%
25	8.31	10	0.19%
25	8.31	12	0.37%
25	8.31	14	0.19%
5	1.38	7	6.89%
5	1.38	11	3.45%
7.1	1.67	5	5.99%
7.1	1.67	8	11.98%

3.2.2 Ultimate loads during operation

A set of load cases belonging to DLC1.6, with normal turbulence class C and severe sea states, for the combinations (v_0, H_s, T_p) given in Table 9 was applied. The chosen periods are all below the natural periods of the system.

Table 9 - Environmental conditions for DLC 1.6.

V_{hub} [m/s]	H_s [m]	T_p [s]
5	15.6	12
5	15.6	14
5	15.6	16
5	15.6	18
7.1	15.6	12
7.1	15.6	14
7.1	15.6	16
7.1	15.6	18
10.3	15.6	12
10.3	15.6	14
10.3	15.6	16
10.3	15.6	18
13.9	15.6	12
13.9	15.6	14
13.9	15.6	16
13.9	15.6	18
17.9	15.6	12
17.9	15.6	14
17.9	15.6	16
17.9	15.6	18
22.1	15.6	12
22.1	15.6	14
22.1	15.6	16
22.1	15.6	18
25	15.6	12
25	15.6	14
25	15.6	16
25	15.6	18

3.2.3 Extreme waves with parked turbine

Parked or idling turbine, $v_0 = 56$ m/s and extreme sea state with H_s=15.6 m and T_p=12, 14, 16 and 18 s.

3.2.4 Extreme wind gust with operating turbine

Wind with extreme operational gust (EOG) and normal sea state.

4 Results

The results of the simplified coupled dynamic models described in Section 1.3 are compared to each other to evaluate their applicability. Here, the suitability of the models in different design load cases can be evaluated. The results have been compared to the state-of-the-art tool FAST v8 that has been set up for the LIFES50+ project with the DTU 10MW RWT in [22], see [23]. It should be noted that the results above rated wind speed rely on an ad-hoc controller designed specifically for the present

deliverable. Changes to the results above and close to rated wind speed can thus be expected following implementation of a refined controller.

The figures in this chapter have a consistent line style convention for the three different models, QuLA, SLOW and FAST. Additionally, in some figures the linearized version of SLOW has been included. The line styles are summarized in Table 10. The plotted signals include the platform surge displacement at the SWL, x_p, the platform pitch displacement, β_p, the tower-top displacement, x_t, as well as the blade pitch angle, θ, and the rotor speed, Ω. The rotor-effective wind speed v_0 and the wave height η and the tower-base bending moment about the axis perpendicular to the wind speed M_{yT} are shown.

Table 10 - Results line style convention

Model	Line style
QuLA	blue
SLOW (nonlinear)	red
FAST	yellow
SLOW (linearized)	purple

4.1 System identification

In this section the results of the first identification tests described in Chapter 3 are shown.

4.1.1 Eigenanalysis

Table 11 shows an Eigenanalysis of the coupled FOWT without controller (open loop). It has been made with SLOW and QuLA. Since SLOW has in the setup used here no heave DOF that one is only shown for QuLA. The drivetrain mode is overdamped in the open-loop case (without active controller) and is therefore not shown.

Table 11 – Eigenanalysis, no aerodynamic forces.

	Undamped eigen-frequency		Undamped eigenperiods				
Model	QuLA	SLOW	FAST	QuLA		SLOW	
	[Hz]	[Hz]	[s]	[s]	Difference to FAST [%]	[s]	Difference to FAST [%]
Platform surge	0.0058	0.0054	174.0	172.4	0.92	185.19	6.43
Platform heave	0.0599	-	16.7	16.69	0.06	-	-
Platform pitch	0.0398	0.0395	26.47	25.13	5.06	25.32	4.34
Tower-top fore-aft displace-ment	0.4157	0.4065	2.56	2.41	5.86	2.46	3.91

4.1.2 Time-domain

In order to assess transient responses of the structure and the applied models, time-domain simulations are performed and compared to FAST results. These include free-decay simulations, regular wave response and the response to an extreme operational gust (EOG). The free-decay simulations are performed in still water without aerodynamic forcing of the simplified tools QuLA and SLOW and the reference model FAST, see Figure 18 and Figure 19.

Surge decay simulation. As indicated by the eigenanalysis above, the surge natural frequency of SLOW and QuLA is in very good agreement with the FAST surge natural frequency. In the first surge oscillation, Figure 18, the simplified models appear to be less damped than the FAST model. However in subsequent surge oscillations the opposite is true, in particular for QuLA. This is evidence of the nonlinear hydrodynamic viscous damping model utilized in FAST as compared to the linear models used in QuLA and SLOW. The induced pitch motion predicted by all three models are in good agreement. This indicates that couplings between surge and pitch are sufficiently captured by the simplified models. The slight difference in steady state pitch offset is due to the fact that in QuLA the lateral eccentric position of the wind turbine centre of gravity is not considered.

Pitch decay simulation. In the case of pitch decay, Figure 19, similar observations as in surge can be made. In this case there are slightly larger discrepancies between the simplified models and FAST predicted oscillation peaks, which in turn exacerbates the differences in induced surge motion between the models. However these differences are not large and the behaviour of the simplified models in pitch is comparable to the FAST model. The tower-top displacement is less damped for SLOW and QuLA. However, in these simulations no aerodynamic forces are present. These will introduce a damping much larger than the structural damping.

Regular wave simulation. Figure 20 shows the response to regular waves of $T_p = 10$s. QuLA predicts here slightly larger amplitudes in surge and pitch. The wave excitation force models are essentially the same for the three models. All read the frequency-domain wave excitation force vector from WAMIT and convert it to time-domain through an inverse Fourier transform. The larger response of QuLA may be explained by the absence of quadratic viscous damping.

Extreme Operating Gust. The response to an Extreme Operating Gust (EOG) in still water serves well for model verification as it excites the system once, resulting in a decay response of the system. It is shown for the FAST model and the nonlinear and the linearized SLOW model in Figure 21 for 16m/s wind speed. The linearized SLOW model is very useful for so called single-in-single-out (SISO)-control design methods but due to the nonlinearities of the aerodynamic forces and also the structural equations of motion the linearization poses difficulties. The results show that the response compares well between the models. Therefore, the structural modes of the tower, the aerodynamic model, the still-water hydrodynamics and the mooring dynamics can be considered valid also for the linear model and applicable for controller design. The linear model has been used for the design of the controller, see Section 2.4.

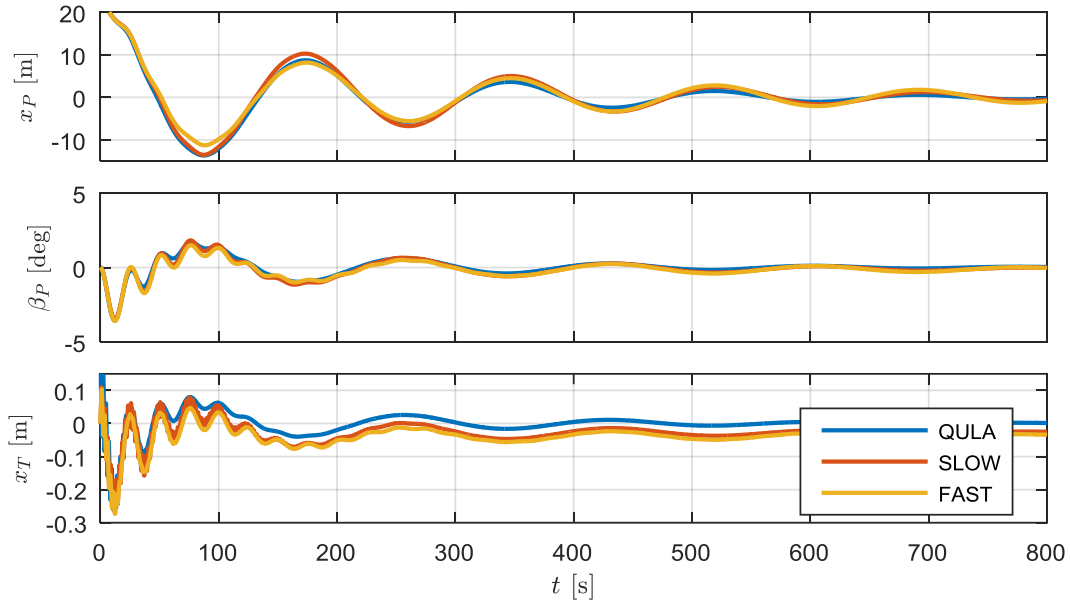

Figure 18 – Surge free-decay.

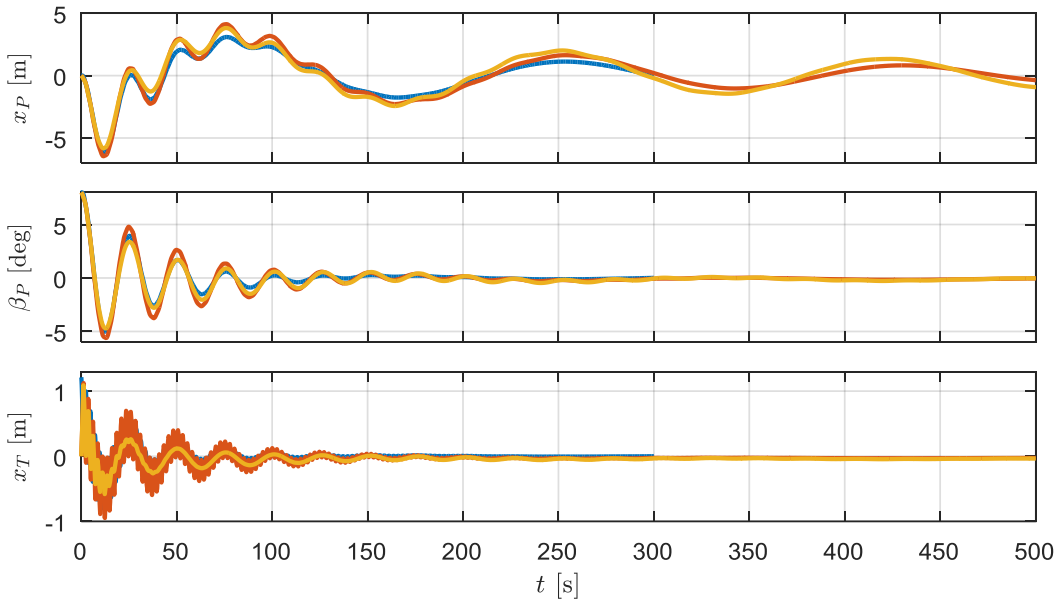

Figure 19 – Pitch free-decay..

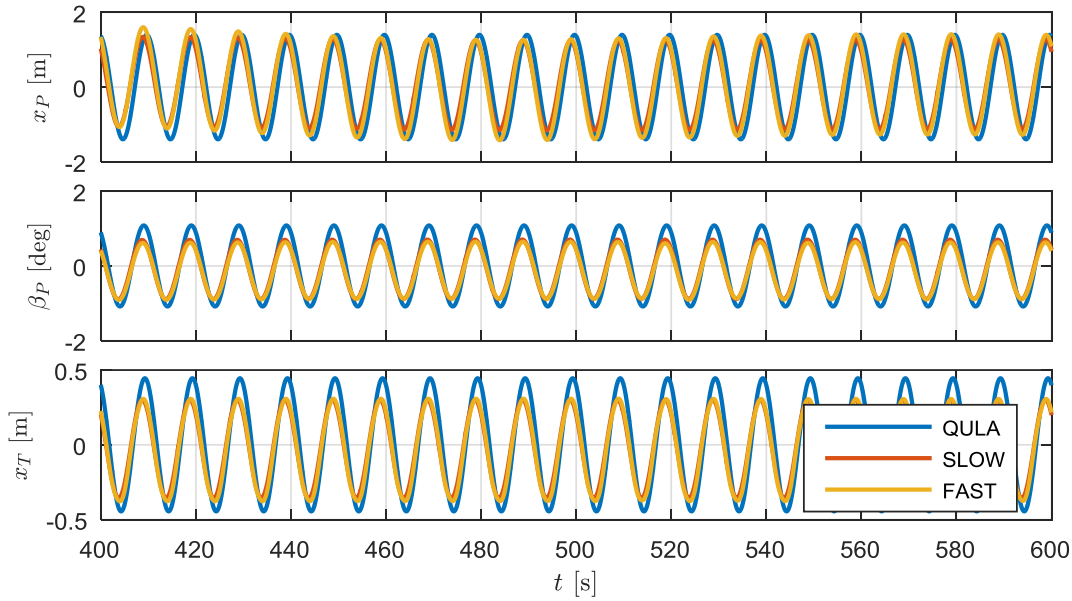

Figure 20 – Regular wave response.

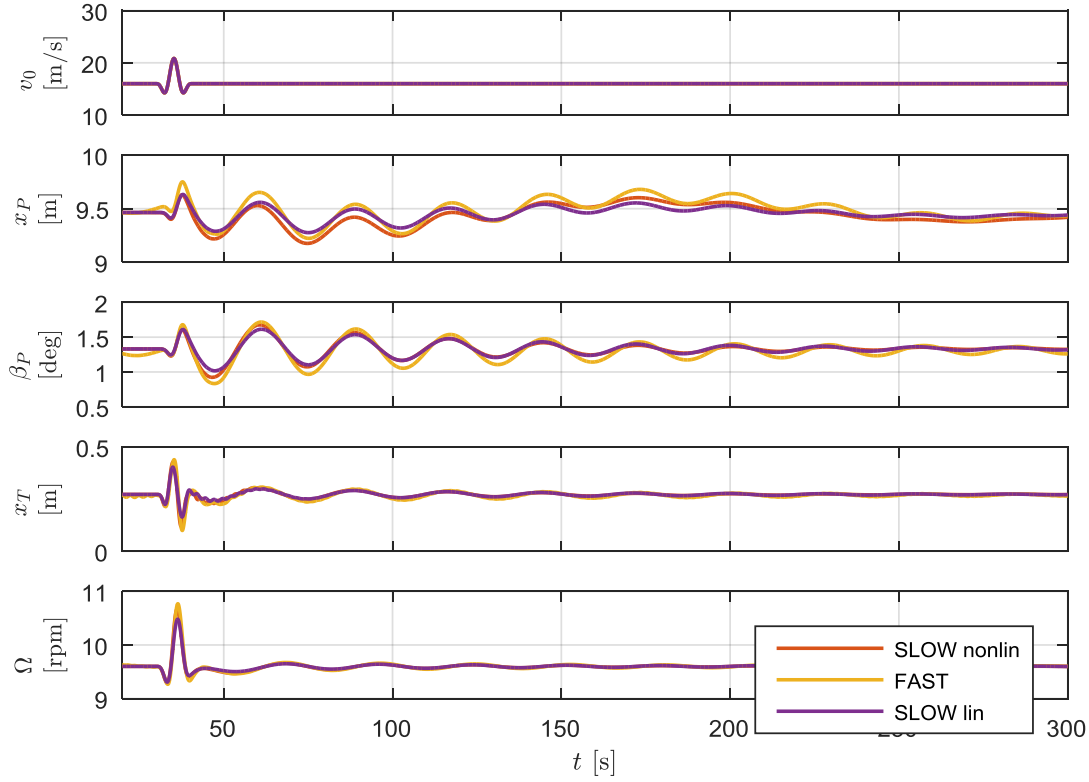

Figure 21 – Linear SLOW model compared to nonlinear and FAST in EOG @ 16m/s.

4.2 Design load cases

The design load cases (DLC) presented in this section are taken from the design basis of LIFES50+ [5]. A selection has been made for this deliverable with a complete operational load case for fatigue analysis and several operational and shut-down conditions for extreme-load analysis. For all design

load cases 1-hour simulations have been performed, where the transient of the first 10min has been cut off for the calculation of statistical values and DELs.

4.2.1 Fatigue loads

In this section DLC 1.2 is evaluated. One above-rated wind speed case has been selected for a time-domain comparison of FAST, SLOW and QuLA, see Figure 22. It can be seen that the magnitudes compare well between the models but also some of the transient features are followed well by the models. The same wave train and wind field has been used for all models.

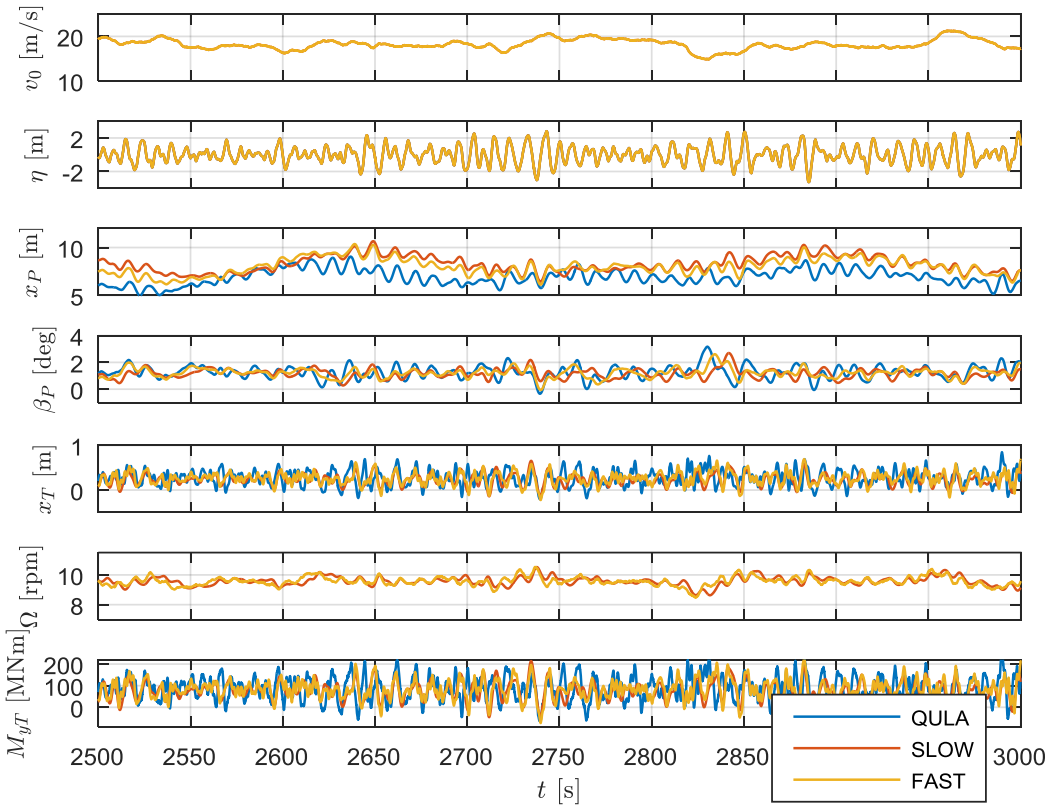

Figure 22 – DLC1.2 time domain comparison 18m/s, Hs=4.3m, Tp=10s.

The difference in response can be explained by the different aerodynamic forcing approaches of the models, see Section 1.3. For a frequency-domain assessment the power-spectral density (PSD) is calculated for the same case of DLC1.2 as for the time-domain comparison, see Figure 24 and for a below-rated case with a different wave peak-spectral period, Figure 23. It shows that for low frequencies the models compare well with the platform surge and pitch modes at 0.005Hz and 0.04Hz. It can be seen that SLOW does not capture the correct magnitude response around the tower mode (0.4Hz). This is due to the fact that the rotor-effective wind speed is used as input to the model, which filters most of the high-frequency turbulence and therefore the tower-mode is not excited in the same way as in FAST. Also the 3p-frequency at 0.48Hz, slightly above the tower eigenfrequency, is not visible for SLOW as the blades are not modelled and effects from e.g. wind shear. QuLA does capture well the 3p-excitation, which is due to the fact that the thrust force timeseries are captured from an onshore simulation with FAST. It shows that although this procedure is not completely "coupled" these effects can be well represented. The first tower frequency is estimated well by QuLA, although the energy content is here overestimated. Furthermore, the damping of QuLA seems to be smaller than in the other models, leading to larger peaks around the tower frequencies in the PSD plot.

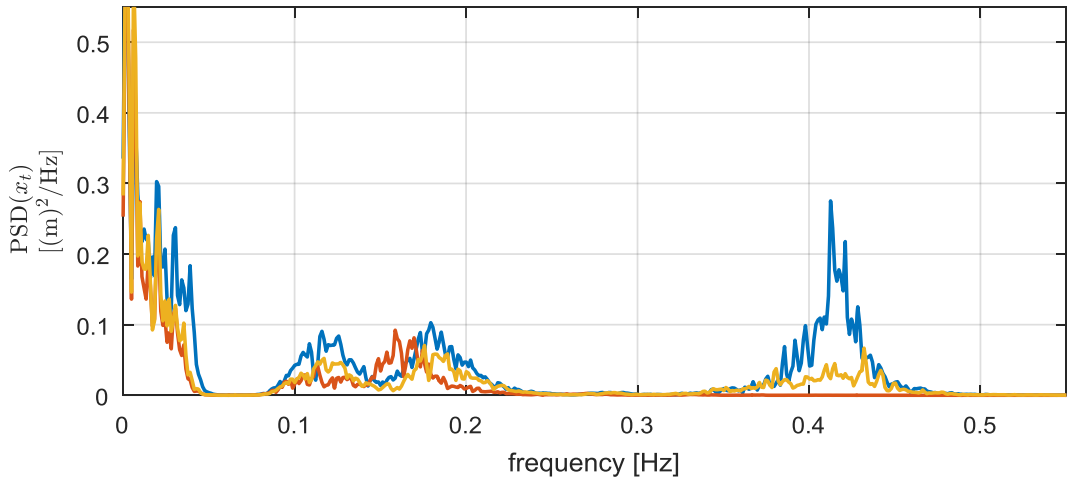

Figure 23 – DLC1.2 PSD comparison tower-top displacement 10m/s, Hs=2.2m, Tp=8s.

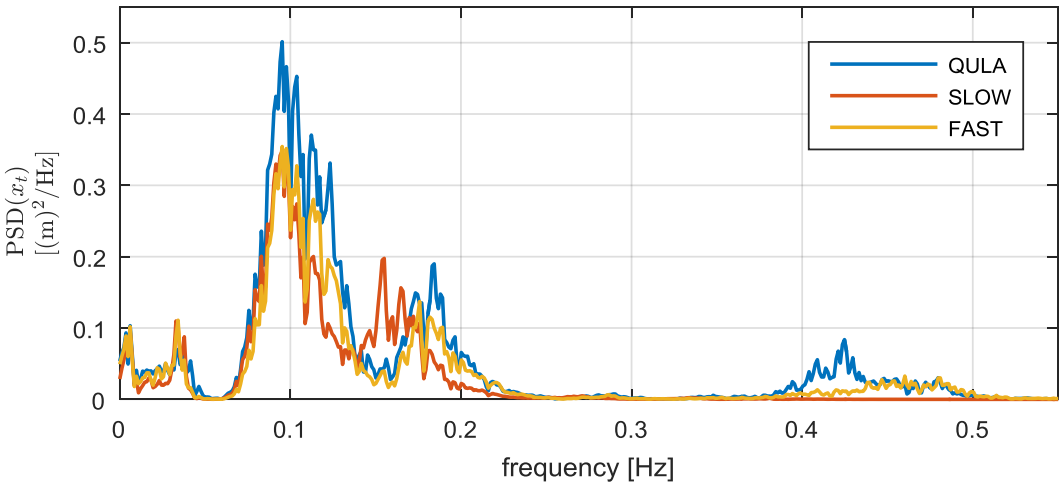

Figure 24 – DLC1.2 PSD comparison tower-top displacement 18m/s, Hs=4.3m, Tp=10s.

The damage equivalent loads of the tower-top fore-aft displacement are compared for three different wave environments as specified in the LIFES50+ design basis [5]. Figure 25, Figure 26 and Figure 27 show a comparison between QuLA, SLOW and FAST over wind speeds for the three wave conditions, shown in Table 8. It can be seen that QuLA overpredicts for most bins, whereas SLOW underpredicts the DELs. One reason for the underprediction of SLOW is the filtering of the high-frequency turbulence in the rotor-effective wind speed as mentioned above. QuLA shows also in the PSD plots above a higher amplitude around the tower eigenfrequency, which might explain the higher DELs compared to FAST.

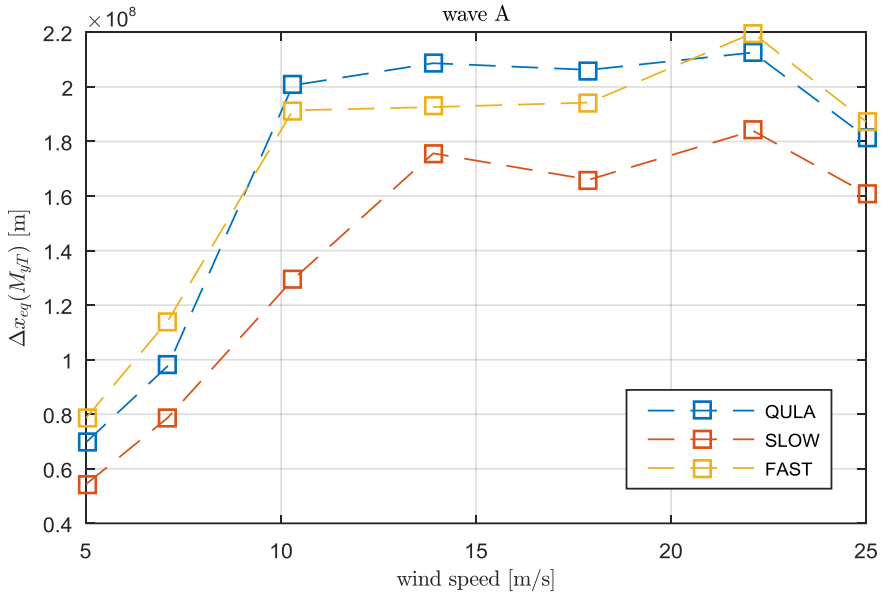

Figure 25 – DLC1.2 tower-base DEL comparison over wind speeds, wave condition A

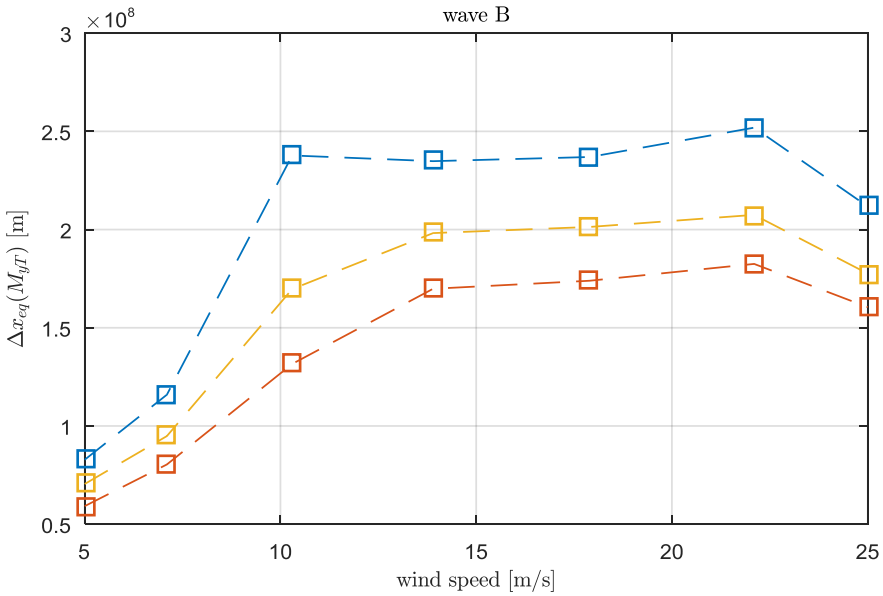

Figure 26 – DLC1.2 tower-base DEL comparison over wind speeds, wave condition B

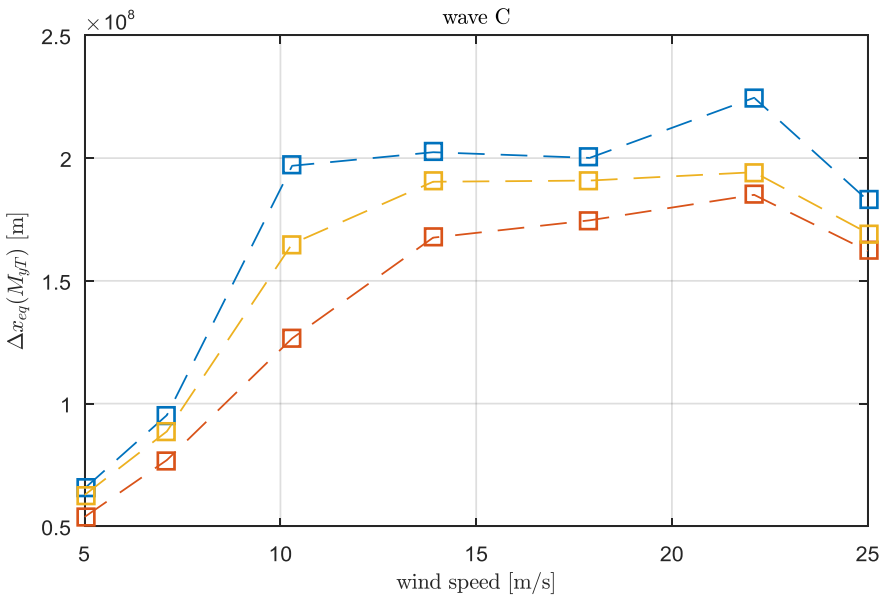

Figure 27 – DLC1.2 tower-base DEL comparison over wind speeds, wave condition C

In a second step the DELs have been weighted with the probability density shown in Table 8 and averaged for the three wave conditions. Figure 28 shows that the weighting stresses wind speeds around rated due to the higher probability of occurrence of these wind speeds.

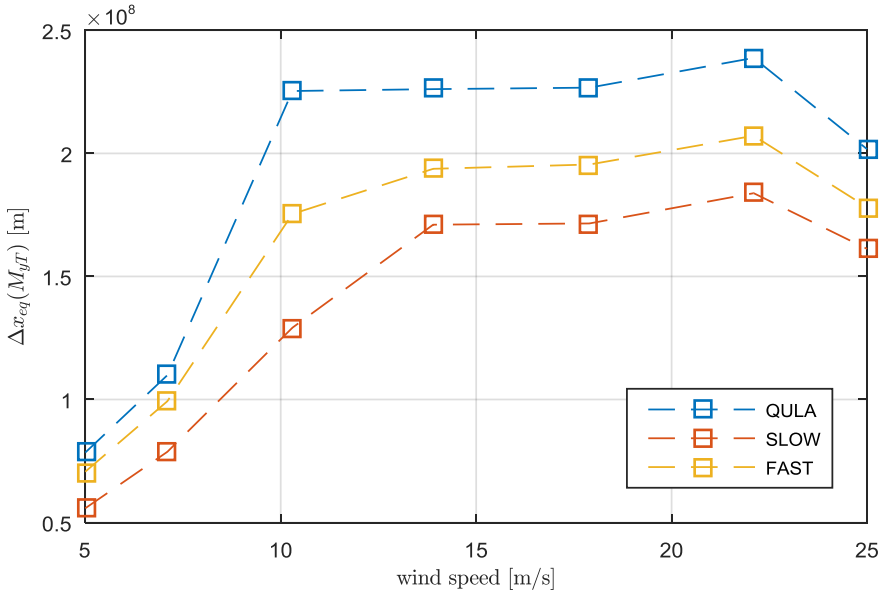

Figure 28 – DLC1.2 weighted tower-base DEL, averaged over wave A, B, C.

The probability of exceedance by the three models is compared in Figure 29 for wave *A* and *C*. The timeseries of the considered signals have been binned based on the zero-upcrossing periods of the wave height signals and the extremes recorded and plotted over their probability of exceedance. Figure 29 shows the platform surge and Figure 30 the tower-top displacement signal. In both figures three wind bins of $v_0 = [10,18,25]$ m/s for wave environments A and C have been compared. Only around rated (10m/s) QuLA predicts smaller extreme values. While SLOW compares well to FAST at $v_0 = 10$ m/s, notable discrepancies occur between FAST and the simplified models in particular for $v_0 = 17.9$ m/s and also at $v_0 = 25$ m/s for wave climate *C*.

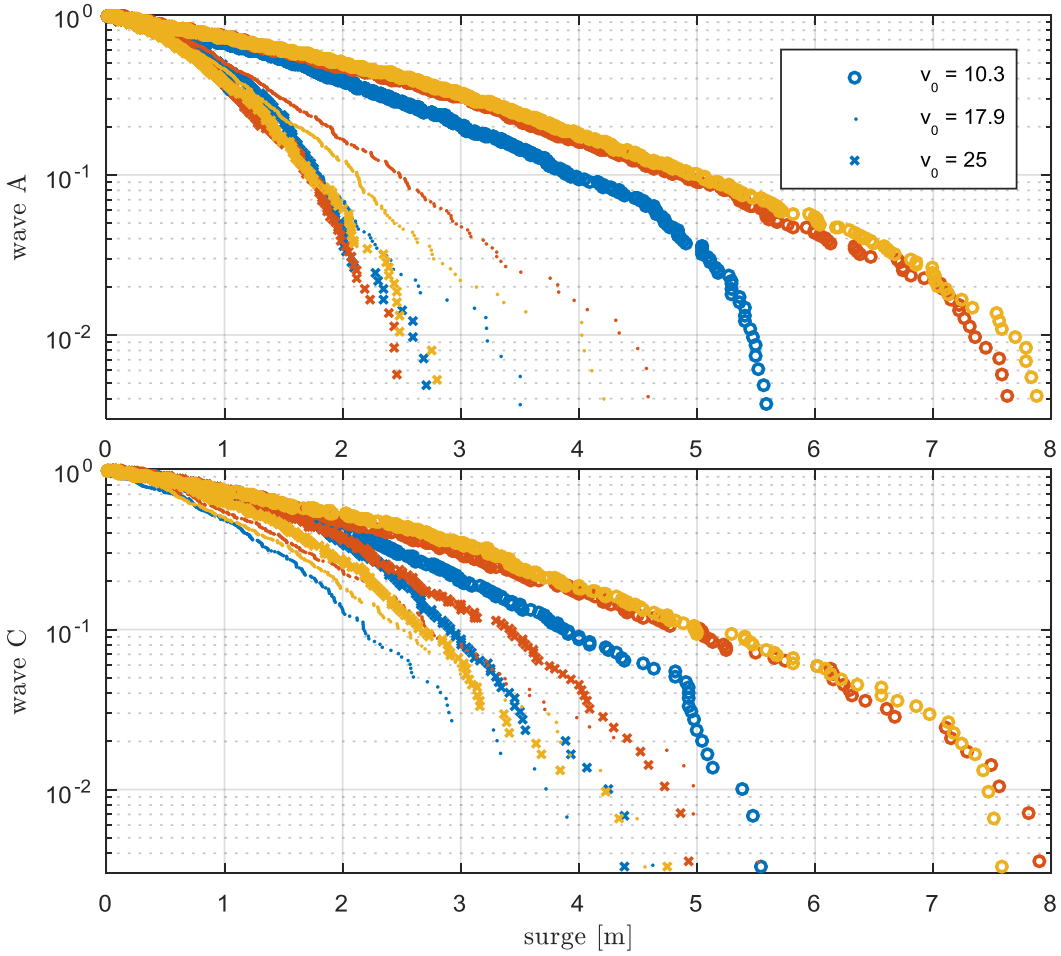

Figure 29 – DLC1.2 platform surge probability of exceedance; wave A, C; v=[10,18,25]m/s; (QuLA-blue, SLOW-red, FAST-yellow).

For the tower-top fore-aft probability of exceedance in Figure 30 one can see a comparable picture to the DEL plots of Figure 28. QuLA overpredicts the amplitudes whereas SLOW underpredicts them.

The probability of exceedance calculation is usually useful for extreme value calculation. However, the plots have been produced here also for a production load case in order to compare them to the extreme load cases in the following. It is mentioned that the motion and load amplitudes assessed in this method depend strongly on the damping. Since SLOW and QuLA only consider linear hydrodynamic damping a large difference appears here although the general dynamics agree. It is again stressed that results above rated wind speed rely on the controller. Hence although model re-calibration is needed to improve the match to the FAST model, the results will also change once the LIFES50+ controller is available in the project.

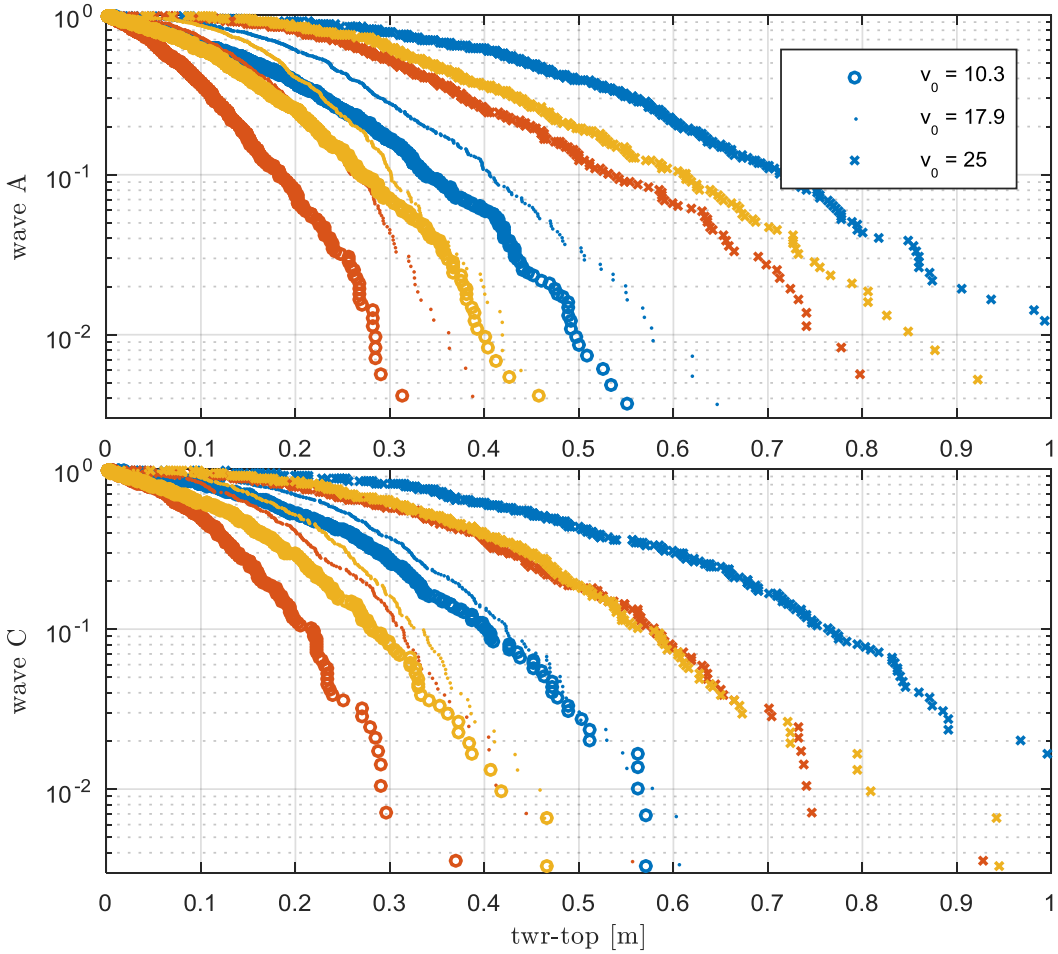

Figure 30 - DLC1.2 tower-top fore-aft probability of exceedance; wave A, C; v=[10,18,25]m/s (QuLA-blue, SLOW-red, FAST-yellow).

4.2.2 Extreme loads

For extreme wave conditions the operational load case DLC1.6 has been considered with 1-hour simulations of each case, resulting in 7 wind speed bins and four wave scenarios and therefore 28 simulations. These conditions are for the most severe site considered in LIFES50+, that of West of Barra.

Figure 31 shows the exceedance probability of platform surge displacement for QuLA, SLOW and FAST. For the large-period case C SLOW overpredicts the motion for wind speed $v_0 = 25$m/s as was seen also above. QuLA overpredicts here the probability for most excursions, although especially for the tower-top displacement the agreement is acceptable.

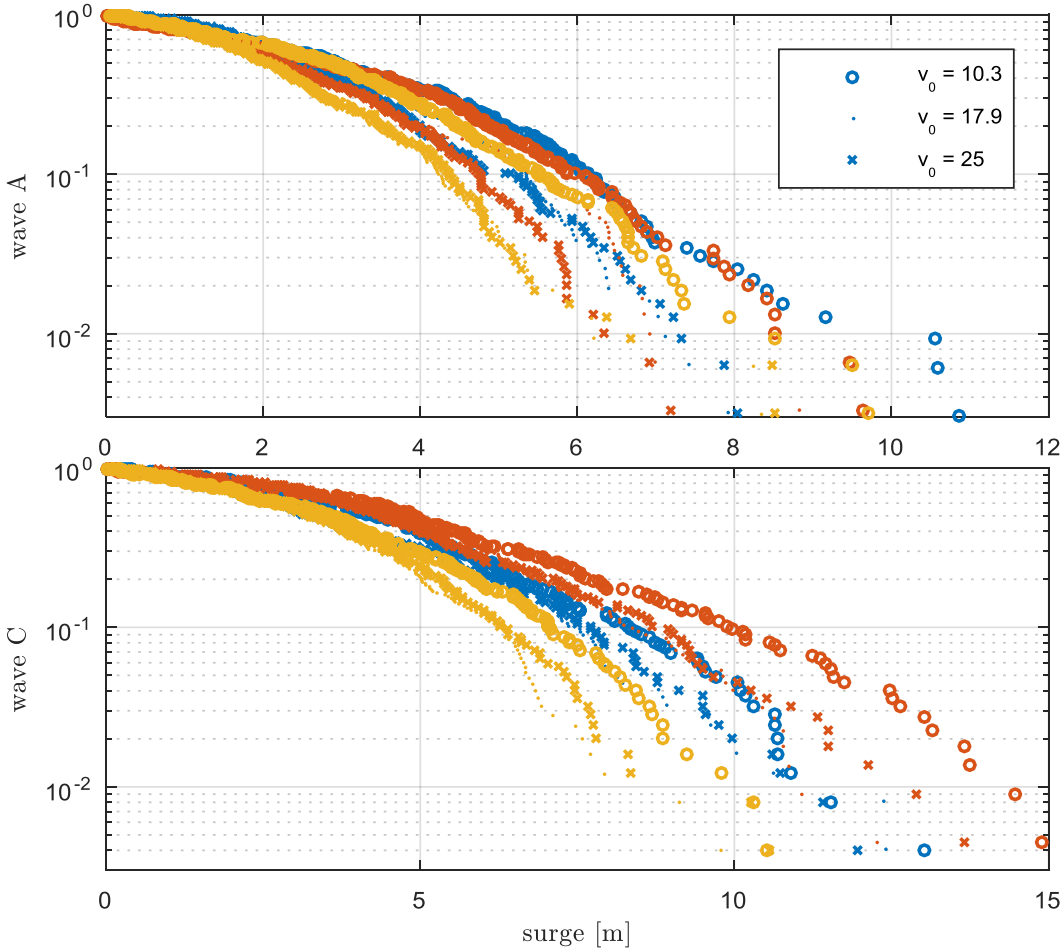

Figure 31 - DLC1.6 platform surge probability of exceedance; wave A, C; v=[10,18,25]m/s (QuLA-blue, SLOW-red, FAST-yellow).

Figure 32 shows the tower-top probability of exceedence of DLC1.6. It can be seen that generally QuLA overpredicts the displacements compared to FAST, whereas SLOW underpredicts them. Again, the results show the ability of the simplified models to predict the correct magnitude of the response, even in a harsh environment. More model tuning can very likely increase the level of accuracy and will be pursued in future work.

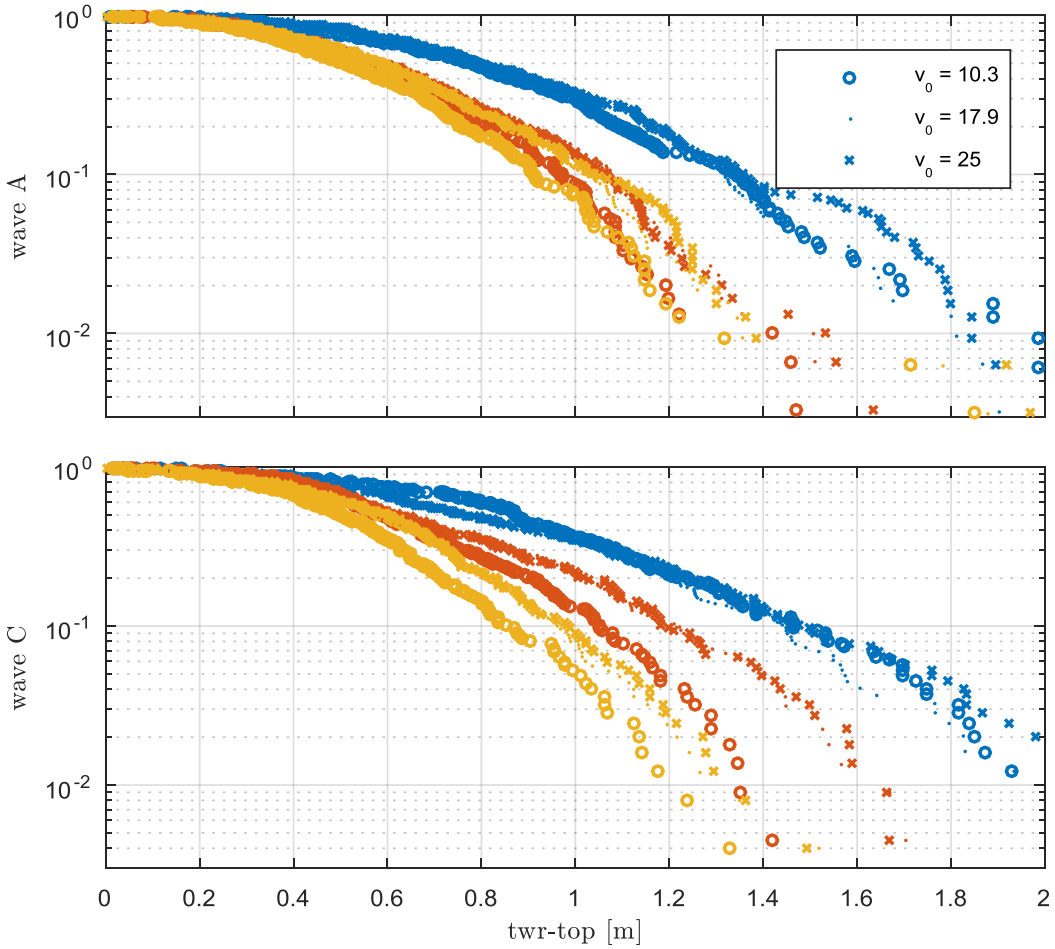

Figure 32 - DLC1.6 tower-top fore-aft probability of exceedance; wave A, C; v=[10,18,25]m/s (QuLA-blue, SLOW-red, FAST-yellow).

Figure 33 shows the probability of exceedance of DLC6.1 where the rotor is idling. The rotor models of FAST and SLOW have been configured such that a viscous brake at the shaft is active and no excessive blade loads occur. It can be seen that there are large discrepancies between the models, which is due to the absence of nonlinear damping in the simple models. For a reliable capturing of the response at these harsh wave environments the models need to be augmented by a more realistic damping model. The first improvement in this regard will be a representation of quadratic viscous damping in QuLA.

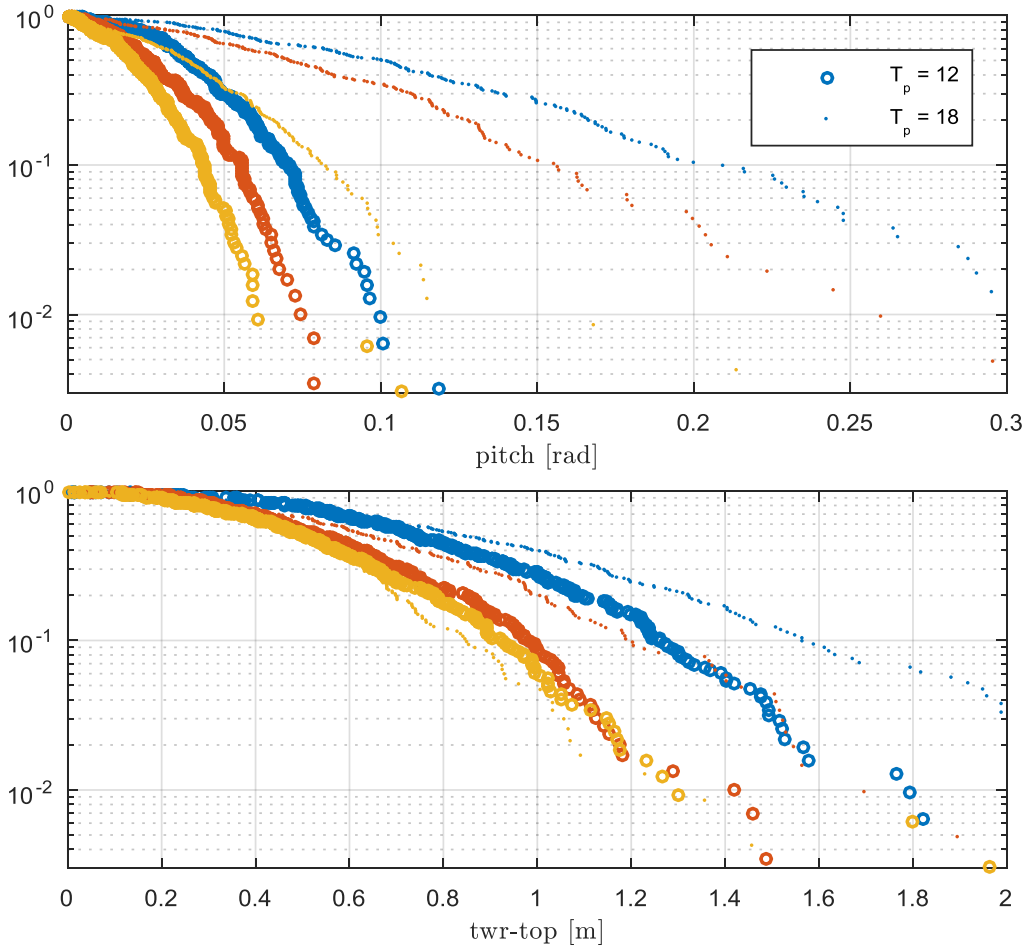

Figure 33 - DLC6.1 platform pitch and tower-top fore-aft probability of exceedance; Tp=[12,18]s (QuLA-blue, SLOW-red, FAST-yellow).

5 Conclusions

The design approach for floating wind turbine substructures considered in this work package promotes utilizing a set of different numerical models covering a range of fidelity and computational efficiency. This report has presented the formulation and assessment of parametric and simplified numerical design tools for use within the conceptual design stage of floating substructures for 10MW wind turbines. SLOW, developed at USTUTT, is a nonlinear coupled numerical model for carrying out fast simulations in the time domain and is particularly aimed at very early design of the floating substructure and wind turbine controller. QuLA, developed at DTU, is a coupled numerical model for evaluating the dynamic response of the floating wind turbine in the frequency domain, with a scope to be more computationally efficient than time-domain simplified numerical models.

The DTU 10MW reference wind turbine installed on the Triple Spar concept was considered as a case study in this work for evaluating a subset of DLCs established in the LIFES50+ Design Basis for the West of Barra site. This site was chosen as it represented the harshest environment available within the LIFES50+ project. Simulations were also carried out using a state-of-the-art FAST model of the floating wind turbine, and were used as a benchmark for results from the simplified numerical models.

It was found that the simplified models were capable of predicting fatigue performance in operating conditions. However, in extreme conditions the simplified numerical models were in limited agreement with the state-of-the-art FAST model. Notable differences were observed, and these are attributed to differences in control, damping and mooring system models within the simplified numerical design tools. Capturing damping related to floating wind turbine aerodynamics is not trivial and as yet no method has been established. The addition of quadratic hydrodynamic damping would contribute to improved performance in extreme conditions. Further, moving beyond a constant-coefficient stiffness matrix to represent the mooring system within QuLA would also contribute to better predicting the dynamic response of the floating wind turbine in extreme conditions. Table 12 presents an overview of the observations made in this work on the applicability of the simplified models for a number of phenomena.

The simplified numerical design tools presented here have the potential to be improved such that their applicability in predicting extreme responses is achieved. This is the subject of future work in work package 4, where advanced numerical tools and experimental results will be used to improve such simplified numerical design tools.

Table 12 - Applicability of simplified models

Phenomena	Applicability for simplified models	Applicability in FAST	Comments
Linear hydrodynamic forces	Yes	Yes	Linear hydrodynamic coefficients (***A***,***B***,***C***) are easy calculated by potential flow theory for large volume bodies or Morison equation for slender bodies. It is easily applied in the model.
Non-linear or 2nd order forces	No	Limited	Higher computational capacity is need to calculate nonlinear effects. It might be possible to estimate these if non diagonal terms from QTF are neglected.
Viscous forces	No	Yes	Viscous phenomena are shown by CFD or tank test
Eigen frequencies	Yes	Yes	It is necessary to be calculated at first stage of design and check possible overlapping with wave frequency range.
Tower frequency modes	Yes	Yes	Some models consider floater structure as a rigid-body, neglecting its elasticity. For initial design is assumable.
Dynamic mooring and export cable design	No	Yes	Slow drift damping forces on the lines in uncertain for simple numerical models. It is difficult to check hull and mooring interaction.
Vortex Induced Motions	No	No	VIM is a strongly non-linear phenomenon and it is difficult to predict it by simple models. Deep draughts columns are usually exposed to VIM.
Identify steady response	Yes	Yes	Simple numerical model, when small amplitude motions happen, are useful to compare and assesassess different preliminary designs
Extreme loads and response	No	Yes	Survival design load cases where high amplitude motions are caused, no linearity is not able to be neglected. Quadratic damping in roll and pitch must be considered.

6 Bibliography

[1] Goren Aguirre and Joannès Berque, "LIFES50+ D7.3: Survey of FOWT Design Practice and Gap Analysis," Tecnalia Foundation, 2015.

[2] Kolja Müller et al., "LIFES50+ D7.4: State-of-the-Art FOWT design practice and guidelines," University of Stuttgart, 2016.

[3] Christian Bak et al., "Description of the DTU 10 MW Reference Wind Turbine," DTU, Tech. rep..

[4] Frank Lemmer, José Azcona, Florian Amann, and Feike Savenije, "INNWIND.EU D4.37 Design Solutions for 10MW Floating Offshore Wind Turbines," INNWIND.EU, 2016.

[5] Antonia Krieger, Gireesh Ramachandran, Luca Vita, Pablo, Berque, Joannès Gómez Alonso, and Goren Aguirre, "LIFES50+ D7.2: Design Basis," DNV-GL, 2015.

[6] Michael Borg and Henrik Bredmose, "LIFES50+ Deliverable 4.4: Overview of the numerical models used in the consortium and their qualification," DTU Wind Energy, 2015.

[7] Jason Jonkman, "Dynamics Modeling and Loads Analysis of an Offshore Floating Wind Turbine," Ph.D. dissertation 2007.

[8] Jason Jonkman, "Definition of the Floating System for Phase IV of OC3," NREL, Tech. rep. 2010.

[9] Frank Sandner, David Schlipf, Denis Matha, Robert Seifried, and Po Wen Cheng, "Reduced Nonlinear Model of a Spar-Mounted Floating Wind Turbine," in *DEWEK*, Bremen, Germany, 2012. [Online]. http://elib.uni-stuttgart.de/opus/volltexte/2013/8439/pdf/Sandner_ReducedModel_Dewek2012.pdf

[10] Denis Matha, Frank Sandner, and David Schlipf, "Efficient critical design load case identification for floating offshore wind turbines with a reduced nonlinear model," , vol. 555, dec 2014. [Online]. http://stacks.iop.org/1742-6596/555/i=1/a=012069?key=crossref.2cf58ea90e06a51553c9c6441bd0248d

[11] Frank Lemmer, Steffen Raach, David Schlipf, and Po Wen Cheng, "Prospects of Linear Model Predictive Control on a 10MW Floating Wind Turbine," in *Proceedings of the ASME 34th International Conference on Ocean, Offshore and Arctic Engineering*, St. John's/Canada, 2015. [Online]. http://elib.uni-stuttgart.de/opus/volltexte/2015/9895/

[12] David Schlipf et al., "Nonlinear Model Predictive Control of Floating Wind Turbines," , 2013, pp. 1-9. [Online]. http://elib.uni-stuttgart.de/opus/volltexte/2013/8516/pdf/13TPC_987Schlipf.pdf

[13] Hansen Craig and David J. Laino, "User's Guide to the Wind Turbine Aerodynamics Computer Software AeroDyn," Tech. rep..

[14] Michael Borg, "Mooring system analysis and recommendations for the INNWIND Triple Spar concept.," Technical University of Denmark, Lyngby, Denmark, DTU Wind Energy Report-I-

0448 2016.

[15] T. J. Larsen and T. D. Hanson, "A method to avoid negative damped low frequent tower vibrations for a floating, pitch controlled wind turbine," Journal of Physics: Conference Series, 75, 012073. doi:10.1088/1742-6596/75/1/012073,.

[16] Gijs Van Der Veen, Yan Couchman, and Robert Bowyer, "Control of floating wind turbines," in *Proceedings of the American Control Conference ACC*, 2012, pp. 3148-3153.

[17] Boris Fischer, "Reducing rotor speed variations of floating wind turbines by compensation of non-minimum phase zeros," , EWEA 2012, 2012.

[18] Jason Jonkman, S Butterfield, W Musial, and G Scott, "Definition of a 5-MW Reference Wind Turbine for Offshore System Development," NREL, Boulder/USA, 2009.

[19] Amy Robertson et al., "Definition of the Semisubmersible Floating System for Phase II of OC4," Tech. rep..

[20] Amy Robertson, "Introduction to the OC5 Project," in *EERA Deepwind*, Trondheim/NO, 2015. [Online]. http://www.sintef.no/Projectweb/Deepwind_2015/Presentations/

[21] Jason Jonkman and Bonnie Jonkman. (2016, March) NWTC Information Portal (FAST v8). [Online]. https://nwtc.nrel.gov/FAST8

[22] Michael Borg, Mahmood Mirzaei, and Henrik Bredmose, "LIFES50+ D1.2 Wind turbine models for the design," 2016.

[23] Michael Borg, "Generic floating substructure configuration and numerical models for wind turbine controller tuning in LIFES50+," Technical University of Denmark, Lyngby, Denmark, DTU Wind Energy Report-I-0449 2016.

7 Checklist for Deliverables

The checklists are created following section 5.2 "LIFES50+ Deliverable Review Procedure" in the Handbook management procedures D9.2.

7.1 Time table

T denotes the submission time point. Unless agreed otherwise the term "delivery in month *n*" means "received by the recipient at 12:00 CET on the last workday in the project month *n"*, where month 1 is June 2015.

✓	When?	Who?	What?	Where to?
✓	T - 2 months	WP leader/Lead beneficiary	Name peer reviewers for deliverable	PM
✓	T - 1 month	Lead beneficiary	Submit advanced draft or full deliverable	PM / Peer Reviewers
✓	T – 2 weeks	Peer Reviewers	Submit feedback on deliverable	Lead beneficiary
☐	T – 2 workdays	WP leader/Lead beneficiary	Upload final version (Word) to project-internal website: http://www.lifes50plus.eu/project	Internal website
☐	T	AST	Final approval by PM Submission to European Committee	EC

7.2 Quality assurance checklist

Checkpoint	✓
Appearance should be generally appealing and according to the LIFES50+ template.	✓
The executive summary should give a short and to the point description of deliverable.	✓
All abbreviations should be explained in footnotes or in a separate list.	✓
All references should be identified and listed.	✓
The deliverable must clearly identify all contributions from partners. It must justify the resources used.	✓
The deliverable must clearly identify the contributions to the state of art. It must justify the scientific contributions.	✓
Each QA check should be signed off in the Document information on page 2.	✓
A full spell check should be completed.	✓